This article has been accepted for publication in IEEE Transactions on Automatic Control. This is the author's version which has not been fully edited and content may change prior to final publication. Citation information: DOI 10.1109/TAC.2024.3399629

Delay-Adaptive Boundary Control of Coupled Hyperbolic PDE-ODE Cascade Systems

Ji Wang and Mamadou Diagne

***Abstract*—This paper presents a delay-adaptive boundary control scheme for a 2×2 coupled linear hyperbolic PDE-ODE cascade system with an unknown and arbitrarily long input delay. To construct a nominal delay-compensated control law, assuming a known input delay, a three-step backstepping design is used. To build the delay-adaptive boundary control law, the nominal control action is fed with the estimate of the unknown delay, which is generated from a batch least-squares identifier that is updated by an event-triggering mechanism that evaluates the growth of the norm of the system states. As a result of the closed-loop system, the actuator and plant states can be regulated exponentially while avoiding Zeno occurrences. The prescribed-time identification of the unknown delay is also achieved. As far as we know, this is the first delay-adaptive control result for systems governed by heterodirectional hyperbolic PDEs. The effectiveness of the proposed design is demonstrated in the control application of a deep-sea construction vessel with cable-payload oscillations and subject to input delay.**

***Index Terms*—Hyperbolic PDEs, delay-adaptive control, event-triggered control, least-squares identifier.**

I. Introduction

A. Boundary control of coupled hyperbolic PDEs

Systems of transport partial differential equations (PDEs) appear in many physical models, including road traffic [26], [64], [65], water management systems [20], [21], [45], [46], flow of fluids in oil drilling systems [14], [27], [28], and cable vibration dynamics [53], [60]. As a result of the backstepping design [15], [52], the sliding mode control approach [40] and the proportional-integral (PI) controller design [51], the theoretical results on boundary control of coupled first-order linear hyperbolic PDEs have emerged in the last decade. The backstepping design was further extended to that of a $n+1$ system in [44], and then to a more general coupled transport PDE system where the number of PDEs in either direction is arbitrary [30]. Along the same lines, studies on the design of an adaptive estimation framework have been proposed in [2], [3] and extended to adaptive control in [6]. However, the problem of delay-adaptive control for hyperbolic PDEs has gone unanswered in all these last developments as traditional designs based on swapping identifiers, passive identifiers, and Lyapunov functions remain difficult to exploit for such systems.

Ji Wang is supported by the National Natural Science Foundation of China under Grant 62203372 and by the Science and Technology Projects of Innovation Laboratory for Sciences and Technologies of Energy Materials of Fujian Province (IKKEM) under Grant HRCP-[2022]-69. Mamadou Diagne is supported by the by NSF CAREER award CMMI-2302030 and NSF grant CMMI-2222250.

J. Wang is with the Department of Automation, Xiamen University, Xiamen, Fujian 361005, China (e-mail:jiwang9024@gmail.com).

M. Diagne is with the Department of Mechanical and Aerospace Engineering, University of California San Diego, 9500 Gilman Dr, La Jolla, CA 92093 (mdiagne@ucsd.edu).

B. Delay-compensated control of finite- and infinite-dimensional plants

Time delays, which are well known to be detrimental to stability [25], often exist in practical control systems. In order to compensate for arbitrarily long delays, "avant-garde" backstepping-based delay compensation techniques were first developed in [35], [37]. Bottom-line, the input delay is converted into a transport PDE as an infinite-dimensional representation of the actuator state. For ODE plants, a PDE/ODE cascade system ensues from this substitute representation of the actuator state. The method has also been used to compensate for the effect of sensor delays that oftentimes occur in ODE plants. In comparison to many results [1], [13], [24], which only estimate plant states, the approach proposed in [35], [37] enables estimation of both the plant and the sensor states when designing a feedback loop. A number of results considering delays that are described by complex transport actuation paths for nonlinear ODE plants were developed in [18], [19] and the references therein.

While compensation for arbitrarily long delays is commonly available for finite-dimensional systems, only very few examples for infinite-dimensional systems were presented, where one pioneering result is [36] that is conceived using backstepping. In recent years, researchers from the PDE control community have shifted their attention to this topic, leading to many interesting developments that can be found in [34], [41], [42], [48], [50]. By treating the delay as a transport PDE, [38] presented the design of a boundary controller for a pure wave PDE with compensation of an arbitrarily long input delay while ensuring exponential stability for the closed-loop system. For coupled heterodirectional hyperbolic PDEs, in [54], a delay-compensated control scheme was designed for a sandwich hyperbolic PDE in the presence of a sensor delay of arbitrary length. In the same spirit, [49] proposed a distributed input delay compensation for traffic systems governed by coupled hyperbolic PDEs (see [47] as well). In addition to the continuous-in-time control law, on the basis of the event-triggered boundary control design of PDEs [23], [22], [55], an event-triggered delay-compensated boundary control law for coupled hyperbolic PDEs was presented in [57]. Although the above substantial results emblematize a major step in the field, the prior knowledge of the delay length is a mandatory weakening factor that mitigates their viability for many practical applications.

Lyapunov designs have been employed to develop delay-adaptive controllers for linear and nonlinear ODE plants [9], [11], [12], [66], [67], [39] via backstepping-based certainty-equivalence compensators. The primary idea behind these contributions is to estimate the unknown delay using input-output signals, and then adjust a pre-designed nominal controller based on estimated parameters in order to achieve convergence. In general, compared to other traditional parameter identifier methods like swapping or passive identifiers, the Lyapunov technique provides better transient performance properties. Recently, the approach has been extended to linear reaction-diffusion PDEs with a boundary or a distributed delayed input [61], [62], where asymptotic convergence results are achieved. In the realm of advancing the design approach of [61], [62], a recent result has achieved the design of Lyapunov-based delay-adaptive boundary control for a scalar Integral PDE [63]. As far as we are aware, the three preceding contributions are the sole results on delay-adaptive control for PDE plants. The method in the present contribution is different with both the above delay-adaptive control results and traditional adaptive control designs for hyperbolic PDEs [6]. More precisely, our design relies on a triggered batch least-square identifier (BaLSI), a novel approach that was initially introduced in [31], [32], which has at least two significant advantages over the traditional adaptive control approaches: guaranteeing exponential regulation of the states to zero, as well as finite-time convergence of the estimates to the true values. This method has been applied in adaptive control of a parabolic PDE [33], and first-order hyperbolic PDEs in [56], [58], [59] with unknown plant parameters.

C. Contributions

- Different with the delay-robust stabilizing feedback control design for coupled first-order hyperbolic PDEs that achieve robustness to small delays in actuation [8], the present contribution ensures exact compensation of the arbitrarily large unknown input delay.
- Exact identification of the unknown delay before the prescribed time is achieved. As a result, the exponential regulation, instead of the asymptotic one in [61], [62], is guaranteed in the closed-loop system. Basically, after the prescribed-time identification of the unknown parameter, the delay-adaptive control signal is identical to the nominal control action (with known input delay), which ultimately improves substantially the resulting transient performance of the whole closed-loop system's dynamics.
- To the best of our knowledge, our result is the first delay-adaptive controller for coupled hyperbolic PDEs involving an unknown and arbitrarily large input delay. In the context of adaptive control of first-order hyperbolic PDEs with unknown transport speeds, as compared to [4], [5], [56], in our work the system cascaded to the first-order hyperbolic PDE capturing actuation delay is a class of coupled hyperbolic PDEs-ODE systems, which is much more complicated than [4], [5], [56] where the cascaded system is a specific scalar ODE or none, and moreover, the finite-time identification is improved to the prescribed-time identification of the unknown transport speed.

D. Organization

The problem formulation is shown in Section II. The nominal control design is presented in Section III. The design of delay-adaptive control with piecewise-constant parameter identification is proposed in Section IV. The main result including the absence of a Zeno phenomenon, parameter convergence, and exponential regulation of the states is proved in Section V. The effectiveness of the proposed design is illustrated with a numerical simulation of a deep-sea construction vessel (DCV) in Section VI. The conclusion and future work are presented in Section VII.

E. Notation

We adopt the following notation.

- The symbol $\mathbb{Z}^+$ denotes the set of natural numbers including zero, and the notation $\mathbb{N}$ for the set $\{1,2,\cdots\}$, i.e., the natural numbers without 0. We also use $\mathbb{R}_+ := [0,+\infty)$.
- Let $U \subseteq \mathbb{R}^m$ be a set with non-empty interior and let $\Omega \subseteq \mathbb{R}$ be a set. By $C^0(U;\Omega)$, we denote the class of continuous mappings on U, which takes values in Ω. By $C^k(U;\Omega)$, where $k \geq 1$, we denote the class of continuous functions on U, which have continuous derivatives of order k on U and take values in Ω.
- We use the notation $L^2(0,1)$ for the standard space of the equivalence class of square-integrable, measurable functions defined on $(0,1)$ and $\|f\| = \left(\int_0^1 f(x)^2 dx\right)^{\frac{1}{2}} < +\infty$ for $f \in L^2(0,1)$.
- For an $I \subseteq \mathbb{R}_+$, the space $C^0(I;L^2(0,1))$ is the space of continuous mappings $I \ni t \mapsto u[t] \in L^2(0,1)$.
- Let $u : \mathbb{R}_+ \times [0,1] \to \mathbb{R}$ be given. We use the notation $u[t]$ to denote the profile of u at certain $t \geq 0$, i.e., $(u[t])(x) = u(x,t)$, for all $x \in [0,1]$.

II. Problem Formulation

Consider the potentially open-loop unstable plant governed by the following 2×2 linear hyperbolic PDE coupled with a linear ODE,

$$\dot{X}(t) = AX(t) + Bw(0,t), \tag{1}$$

$$z_t(x,t) = -q_1 z_x(x,t) + d_1 z(x,t) + d_2 w(x,t), \tag{2}$$

$$w_t(x,t) = q_2 w_x(x,t) + d_3 z(x,t) + d_4 w(x,t), \tag{3}$$

with the boundary conditions:

$$z(0,t) = CX(t) - pw(0,t), \tag{4}$$

$$w(1,t) = c_0 U(t-D) + qz(1,t), \tag{5}$$

where, $q, q_1, q_2, d_1, d_2, d_3, d_4, c_0$ and p are arbitrary parameters with $q_1, q_2 > 0$ being transport speeds, and $p \neq 0$, $c_0 \neq 0$. Here, the matrix A, B, C are known, $z(x,t)$ and $w(x,t)$ are the PDE state variables, $X(t) \in \mathbb{R}^m$ is the linear ODE state, U is the control variable and $D > 0$ is the indiscriminately large and unknown input delay. We assume that the initial conditions satisfy

$$z^0(x), w^0(x) \in L^2(0,1),\ X^0 \in \mathbb{R}^m \tag{6}$$

and consider the following assumptions.

Assumption 1: The pair A, B is controllable.

Assumption 2: Parameters p, q satisfy

$$|pq| e^{\max\left\{\frac{2d_4}{q_2}, \frac{2d_1}{q_1}\right\}} < \frac{1}{\sqrt{2}}. \tag{7}$$

Assumption 3: The bounds of the unknown input delay D are known and arbitrary, i.e.,

$$0 < \underline{D} \le D \le \overline{D} \tag{8}$$

where positive constants $\underline{D}$, $\overline{D}$ are arbitrary.

Our goal is to design a delay-adaptive boundary control action, $U(t)$, that exponentially regulates the system (1)–(5) despite the presence of an unknown delay D whose length is arbitrary. The plant (1)–(5) can be used to model cable-payload oscillations in DCV, which are to be suppressed for the purpose of accurate placement of the equipment to be installed on the sea floor. From this application perspective, large-distance signal transmission in the water through a set of acoustics devices and the actuation of the hydraulic actuator for the ship-mounted crane are subject to delays, which are considered as an unknown delay in the control input, the cable vibration dynamics are governed by the 2×2 hyperbolic PDE, and the vibration dynamics of the cage are captured by the ODE system.

III. Nominal delay-compensated control design

In order to design the nominal control law, we first construct an infinite-dimensional representation of the actuator state by converting the delayed input into transport PDE actuation dynamics. Define a new variable $v(x,t)$ as

$$v(x,t) = \begin{cases} U(t-Dx) & \text{if } t-Dx \ge 0 \\ 0 & \text{if } t-Dx < 0 \end{cases}$$

then (5) is rewritten as

$$w(1,t) = c_0 v(1,t) + qz(1,t), \tag{9}$$

$$v_t(x,t) = -\frac{1}{D} v_x(x,t), \tag{10}$$

$$v(0,t) = U(t), \tag{11}$$

$$v(x,0) = 0 \tag{12}$$

for $x \in [0,1], t \in [0,\infty)$. Now, resulting from the new representation of the actuator state, the function $U(t)$, which is defined as the boundary condition (11) of the transport equation (10), is the delay-free control input to be designed for the hyperbolic PDE-PDE-ODE cascade system consisting of (1)–(4) combined with (9)–(12).

A. First Step: Backstepping Transformation for the 2×2 Coupled Hyperbolic PDE-ODE

We introduce the following backstepping transformation [43] in order to remove the in-domain coupling destabilizing terms from the 2×2 hyperbolic PDE system consisting of (2), (3) and make the ODE system matrix Hurwitz:

$$\alpha(x,t) = z(x,t) - \int_0^x \phi(x,y) z(y,t)dy - \int_0^x \varphi(x,y) w(y,t)dy - \gamma(x)X(t), \tag{13}$$

$$\beta(x,t) = w(x,t) - \int_0^x \Psi(x,y) z(y,t)dy - \int_0^x \Phi(x,y) w(y,t)dy - \lambda(x)X(t) \tag{14}$$

whose inverse is

$$z(x,t) = \alpha(x,t) - \int_0^x \bar{\phi}(x,y)\alpha(y,t)dy - \int_0^x \bar{\varphi}(x,y)\beta(y,t)dy - \bar{\gamma}(x)X(t), \tag{15}$$

$$w(x,t) = \beta(x,t) - \int_0^x \bar{\Psi}(x,y)\alpha(y,t)dy - \int_0^x \bar{\Phi}(x,y)\beta(y,t)dy - \bar{\lambda}(x)X(t) \tag{16}$$

to convert (1)–(4), (9) into

$$\dot{X}(t) = A_{\rm m}X(t) + B\beta(0,t), \tag{17}$$

$$\alpha(0,t) = -p\beta(0,t), \tag{18}$$

$$\alpha_t(x,t) = -q_1\alpha_x(x,t) + d_1\alpha(x,t), \tag{19}$$

$$\beta_t(x,t) = q_2\beta_x(x,t) + d_4\beta(x,t), \tag{20}$$

$$\beta(1,t) = c_0 v(1,t) + q\alpha(1,t) + \left(\bar{\lambda}(1) - q\bar{\gamma}(1)\right)X(t) + \int_0^1 \left(\bar{\Psi}(1,y) - q\bar{\phi}(1,y)\right)\alpha(y,t)dy + \int_0^1 \left(\bar{\Phi}(1,y) - q\bar{\varphi}(1,y)\right)\beta(y,t)dy. \tag{21}$$

The gain vector K is selected so that

$$A_{\rm m} = A + BK^T \tag{22}$$

is Hurwitz.

The conditions on the kernels $\phi(x,y)$, $\varphi(x,y)$, $\gamma(x)$, $\Psi(x,y)$, $\Phi(x,y)$, $\lambda(x)$ and $\bar{\phi}(x,y)$, $\bar{\varphi}(x,y)$, $\bar{\gamma}(x)$, $\bar{\Psi}(x,y)$, $\bar{\Phi}(x,y)$, $\bar{\lambda}(x)$ in the backstepping transformations (13)–(16), which are obtained by matching the original system (1)–(5) and the intermediate system (17)–(21), are shown in the part 1 of Appendix A, and the well-posedness of the kernel conditions has been proved in Theorem 4.1 of [43].

B. Second Step: Transformation of the Actuator States

With the purpose of removing the integral terms and ODE state $X(t)$ from the PDE boundary condition (21), we define the following change of coordinate

$$u(x,t) = v(x,t) + \int_0^1 K_1(x,y)\alpha(y,t)dy + \int_0^1 K_2(x,y)\beta(y,t)dy + \eta(x)X(t) \tag{23}$$

This article has been accepted for publication in IEEE Transactions on Automatic Control. This is the author's version which has not been fully edited and content may change prior to final publication. Citation information: DOI 10.1109/TAC.2024.3399629

which enables one to map the actuator dynamics given by (10), (11), and (21) into the following equations

$$\beta(1,t) = c_0 u(1,t) + q\alpha(1,t), \tag{24}$$

$$u_t(x,t) = -du_x(x,t) + q_2 K_2(x,1) c_0 u(1,t), \tag{25}$$

$$u(0,t) = U(t) + \int_0^1 K_1(0,y)\alpha(y,t)dy + \int_0^1 K_2(0,y)\beta(y,t)dy + \eta(0)X(t), \tag{26}$$

where

$$d = \frac{1}{D}.$$

The detailed computation and conditions of the kernels $K_1(x,y), K_2(x,y), \eta(x)$ are given in the part 2 of Appendix A.

C. Third Step: Backstepping Transformation for the Resulting u-PDE

To remove the boundary nonlocal term $q_2 K_2(x,1) c_0 u(1,t)$ in the transport PDE (25), we apply the following mapping

$$u(x,t) = \hat{u}(x,t) + \int_x^1 R(x,y)\hat{u}(y,t)dy \tag{27}$$

which converts (24)–(26) into

$$\beta(1,t) = c_0 \hat{u}(1,t) + q\alpha(1,t), \tag{28}$$

$$\hat{u}_t(x,t) = -d\hat{u}_x(x,t), \tag{29}$$

$$\hat{u}(0,t) = 0, \tag{30}$$

with the nominal control input defined as

$$U(t) = -\int_0^1 K_1(0,y;D)\alpha(y,t)dy - \int_0^1 K_2(0,y;D)\beta(y,t)dy + \int_0^1 R(0,y;D)\hat{u}(y,t)dy - \eta(0;D)X(t). \tag{31}$$

The conditions of the kernel $R(x,y)$ are shown in the part 3 of Appendix A. Writing D after ";" in (31) emphasizes the fact that these functions are parameterized by the delay D. The inverse transformation of (27) can be found as

$$\hat{u}(x,t) = u(x,t) + \int_x^1 P(x,y)u(y,t)dy, \tag{32}$$

where the conditions of $P(x,y)$ are given in the part 3 of Appendix A as well.

D. Stability result of nominal delay-compensated control

The flow diagram of the nominal delay-compensated control is shown in Figure 1. In a nutshell, the prior transformations convert the original system that consists of (1)–(4), (9)–(12) into the target system that consists of (17)–(20), (28)–(30). The nominal control input (31) is rewritten with respect to the original state variables as follows

$$U(t) = \int_0^1 M_1(y;D)z(y,t)dy + \int_0^1 M_2(y;D)w(y,t)dy + \int_0^1 M_3(y;D)v(y,t)dy + M_4(D)X(t), \tag{33}$$

where the controller gains M_i, $i = 1,\cdots,4$ are given in Appendix B, which includes the delay D.

The stability result of the nominal delay-compensated control is stated as follows.

Theorem 1: For the known delay D, with arbitrary initial data $(z[0],w[0])^T \in L^2(0,1)$, $X(0) \in \mathbb{R}^m$, considering the closed-loop system consisting of the plant (1)–(4), (9)–(12) and the nominal controller (33), the exponential stability of the closed-loop system is obtained in the sense that there exist positive constants Υ, λ_1 such that

$$\Omega(t) \le \Upsilon\Omega(0)e^{-\lambda_1 t}, \quad t \ge 0, \tag{34}$$

where $\Omega(t)$ is defined as

$$\Omega(t) = \|z[t]\|^2 + \|w[t]\|^2 + \|v[t]\|^2 + |X(t)|^2. \tag{35}$$

Proof: Define Lyapunov function $V(t)$ as

$$V(t) = \frac{r_d}{2}X^T(t)P_1X(t) + \frac{r_a}{2}\int_0^1 e^{\delta x}\beta(x,t)^2dx + \frac{1}{2}\int_0^1 e^{-\delta x}\alpha(x,t)^2dx + \frac{r_c}{2}\int_0^1 e^{-x}\hat{u}(x,t)^2dx, \tag{36}$$

where a positive definite matrix $P_1 = P_1{}^T$ is the solution to the Lyapunov equation $A_{\mathrm{m}}^T P_1 + P_1 A_{\mathrm{m}} = -Q_1$ for some $Q_1 = Q_1{}^T > 0$, and where δ, r_a, r_c, r_d satisfy

$$e^{-2\max\left\{\frac{2d_4}{q_2},\frac{2d_1}{q_1}\right\}} > e^{-2\delta} > 2p^2q^2, \tag{37}$$

$$\frac{q_1}{2q_2q^2}e^{-2\delta} \ge r_a > \frac{p^2q_1}{q_2}, \tag{38}$$

$$r_c \ge 2\bar{D}q_2r_ae^{\delta}c_0^2, \tag{39}$$

$$0 < r_d \le \frac{\lambda_{\min}(Q_1)}{2|P_1B|^2}\left(q_2r_a - p^2q_1\right). \tag{40}$$

Please note that $e^{-2\max\left\{\frac{2d_4}{q_2},\frac{2d_1}{q_1}\right\}} > 2p^2q^2$ holds in (37) under Assumption 2, and $\frac{q_1}{2q_2q^2}e^{-2\delta} > \frac{p^2q_1}{q_2}$ holds in (38) due to the right inequality in (37), which means the existence of δ, r_a satisfying (37), (38). It is then straightforward to obtain r_c, r_d by (39), (40), where the positiveness of the right-hand side of (40) is ensured by the right inequality in (38). Therefore, there exists a solution δ, r_a, r_c, r_d satisfying (37)–(40).

Following the calculation in Appendix D and using the norm estimate (D.10), we have

$$\xi_1\xi_3\Omega(t) \le V(t) \le \xi_2\xi_4\Omega(t) \tag{41}$$

where ξ_1, ξ_2 are given in (D.11), (D.12), and

$$\xi_3 = \frac{1}{2}\min\left\{r_d\lambda_{\min}(P_1), r_a, e^{-\delta}, r_ce^{-1}\right\}, \tag{42}$$

$$\xi_4 = \frac{1}{2}\max\left\{r_d\lambda_{\max}(P_1), r_ae^{\delta}, 1, r_c\right\}, \tag{43}$$

where $\lambda_{\min}(P_1)$ is the smallest eigenvalue of P_1.

Taking the derivative of (36) along (17)–(20), (28)–(30), and applying Young's inequality and the Cauchy-Schwarz inequality, the following estimate holds for all $t \ge 0$:

$$\dot{V}(t) \le -\frac{r_d}{4}\lambda_{\min}(Q_1)|X(t)|^2 - \left(\frac{1}{2}q_1e^{-\delta} - q_2r_ae^{\delta}q^2\right)\alpha(1,t)^2 - \left(\frac{1}{2}q_2r_a - \frac{r_d|P_1B|^2}{\lambda_{\min}(Q_1)} - \frac{p^2q_1}{2}\right)\beta(0,t)^2$$

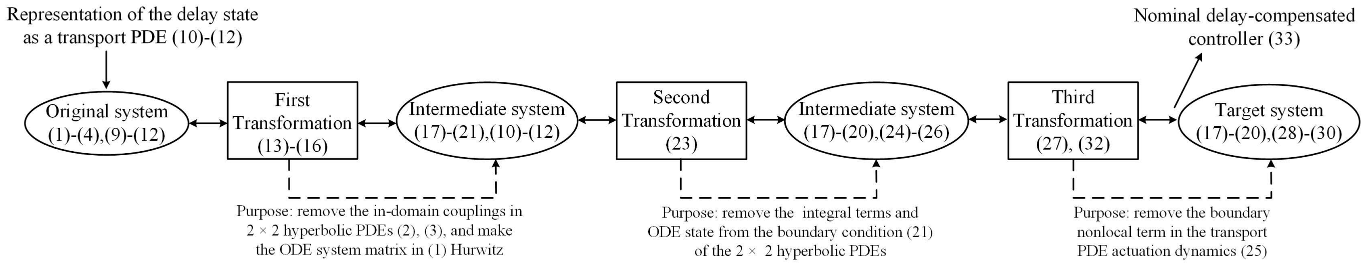

Fig. 1: The flow diagram of the nominal delay-compensated control design.

$$
\begin{aligned}
&-r_a\left(\frac{1}{2}\delta q_2-d_4\right)\int_0^1 e^{\delta x}\beta(x,t)^2dx\\
&-\left(\frac{1}{2}\delta q_1-d_1\right)\int_0^1 e^{-\delta x}\alpha(x,t)^2dx\\
&-\left(\frac{r_c}{2D}-q_2r_ae^{\delta}c_0^2\right)\hat{u}(1,t)^2\\
&-\frac{r_c}{2D}\int_0^1 e^{x}\hat{u}(x,t)^2dx. \qquad (44)
\end{aligned}
$$

Recalling conditions (37)–(39) on δ, r_a, r_c, and r_d, there exists a sufficiently small positive constant λ_1, such that

$$\dot{V}(t)\le-\lambda_1V(t), \qquad (45)$$

where

$$\lambda_1=\min\left\{\frac{\lambda_{\min}(Q_1)}{2\lambda_{\max}(P_1)},\delta q_2-2d_4,\delta q_1-2d_1,\frac{1}{D}\right\}>0. \quad (46)$$

Recalling (41), we then obtain (34) where the positive constant Υ is given as

$$\Upsilon=\frac{\xi_2\xi_4}{\xi_1\xi_3}. \qquad (47)$$

The proof of the theorem is complete. ■

Next, we will design a delay-adaptive controller considering the nominal control action (33) fed with an estimate $\hat{D}$ that is given by an update law resulting from a triggered batch least-square identifier of the unknown delay D.

IV. Delay-Adaptive Control Design

Before presenting the controller, we propose the design of a triggered batch least-squares identifier for the unknown delay, in the following two subsections.

A. Triggering mechanism

The triggering mechanism for the batch least-squares identifier is defined as

$$
t_{i+1}=\begin{cases}\min\Big\{\inf\{t>t_i:\Omega(t)=(1+a)\hat{\Upsilon}(\hat{D}(t_i))\Omega(t_i)\},\\ \qquad t_i+T\Big\}, \qquad for \quad \Omega(t_i)\neq 0\\ t_i+T, \qquad\qquad for \ \Omega(t_i)=0\end{cases} \qquad (48)
$$

where the positive design parameter a is free, another positive design parameter

$$T\le\frac{T_{\rm f}}{2} \qquad (49)$$

is the maximum dwell time between two adjacent triggering time instants, and the free design parameter $T_{\rm f}>0$ is the prescribed time of identifying the unknown delay. The function $\Omega(t)$ is given in (35). The function $\hat{\Upsilon}(\hat{D}(t_i))\ge 1$ is the overshoot coefficient that is associated with the system transient and is obtained by replacing the unknown D with $\hat{D}(t_i)$ in Υ which is defined in (47) (please note that ξ_1 and ξ_2 in (47) depend on the delay D through the delay-dependent kernel functions K_1,K_2,η,R,P included in (D.11) and (D.12). See Appendix D for further details).

B. Least-squares identifier for the unknown delay

Now, we design the identifier which stands as the update law of the estimated delay $\hat{D}$. According to (10), for $\tau>0$ and $n=1,2,\cdots$, the following equality holds:

$$D\frac{d}{d\tau}\int_0^1\sin(x\pi n)v(x,\tau)dx=\pi n\int_0^1\cos(x\pi n)v(x,\tau)dx. \qquad (50)$$

Integrating (50) from 0 to t, yields

$$D\int_0^1\sin(x\pi n)v(x,t)dx=\pi n\int_0^t\int_0^1\cos(x\pi n)v(x,\tau)dxd\tau \qquad (51)$$

where (12) has been recalled. Straightforwardly, (51) can be written as

$$f_n(t)=Dg_n(t), \qquad (52)$$

where

$$f_n(t)=\pi n\int_0^t\int_0^1\cos(x\pi n)v(x,\tau)dxd\tau, \qquad (53)$$

$$g_n(t)=\int_0^1\sin(x\pi n)v(x,t)dx, \qquad (54)$$

for $n\in\mathbb{N}$. Define the function $h_{i,n}$ by the formula:

$$h_{i,n}(\ell)=\int_{\mu_{i+1}}^{t_{i+1}}(f_n(t)-\ell g_n(t))^2dt,\ i\in\mathbb{Z}^+,n\in\mathbb{N}, \qquad (55)$$

and time instant μ_{i+1} as

$$\mu_{i+1}:=\min\{t_g:g\in\{0,\ldots,i\},t_g\ge t_{i+1}-\tilde{N}T\}, \qquad (56)$$

where the positive integer $\tilde{N}\ge 1$ is a free design parameter (in practice, a lager $\tilde{N}$ means a bigger set of data used in the least-squares identifier, which makes the identifier more robust with respect to measurement errors), and where the positive constant T is the maximum dwell time according to

(48). From (52), one can deduce that the function $h_{i,n}(\ell)$ in (55) has a global minimum $h_{i,n}(D)=0$. Then, using Fermat's theorem (vanishing gradient at extrema), the following matrix equation hold for every $i\in\mathbb{Z}^+$ and $n\in\mathbb{N}$:

$$H_n(\mu_{i+1},t_{i+1}) = G_n(\mu_{i+1},t_{i+1})D \tag{57}$$

where

$$H_n(\mu_{i+1},t_{i+1}) = \int_{\mu_{i+1}}^{t_{i+1}} g_n(t) f_n(t)dt, \tag{58}$$

$$G_n(\mu_{i+1},t_{i+1}) = \int_{\mu_{i+1}}^{t_{i+1}} g_n(t)^2 dt. \tag{59}$$

Indeed, (57) is obtained by differentiating the functions $h_{i,n}(\ell)$ defined by (55) with respect to ℓ, and evaluating the derivative (zero) at the global minimum $\ell=D$. Using (57)–(59), the following delay identifier is constructed:

$$\hat{D}(t_{i+1}) = \operatorname{argmin}\Big\{|\ell-\hat{D}(t_i)|^2 : \underline{D}\le\ell\le\overline{D}, \quad H_n(\mu_{i+1},t_{i+1}) = G_n(\mu_{i+1},t_{i+1})\ell, \quad n=1,2,\cdots\Big\}, \quad i\in\mathbb{Z}^+. \tag{60}$$

Remark 1 (Implementation of the identifier): Implementation of the identifier begins with calculating $H_n(\mu_{i+1},t_{i+1})$, $G_n(\mu_{i+1},t_{i+1})$ from $n=1$, $i=0$, i.e., $H_1(\mu_1,t_1)$, $G_1(\mu_1,t_1)$, using (58), (59), (53), (54). If $G_1(\mu_1,t_1)\neq 0$, it implies that ℓ belongs to a singleton set, i.e., $\ell=\frac{H_1(\mu_1,t_1)}{G_1(\mu_1,t_1)}$. It is followed that the output of the identifer (60) at t_1 is $\hat{D}(t_1)=\frac{H_1(\mu_1,t_1)}{G_1(\mu_1,t_1)}$. If $G_1(\mu_1,t_1)=0$, we continue to calculate H,G with $n=2$, $i=0$, i.e., $H_2(\mu_1,t_1)$, $G_2(\mu_1,t_1)$, and then evaluate the value of $G_2(\mu_1,t_1)$. Similarly, if $G_2(\mu_1,t_1)\neq 0$, the output of the identifier at t_1 is $\hat{D}(t_1)=\frac{H_2(\mu_1,t_1)}{G_2(\mu_1,t_1)}$. If $G_2(\mu_1,t_1)=0$, then move to calculate the case of $n=3$, $i=0$, i.e., $H_3(\mu_1,t_1)$, $G_3(\mu_1,t_1)$. Repeating the above steps, until we find a $G_n(\mu_1,t_1)\neq 0$ for a certain n, the output of the identifier at t_1 is $\hat{D}(t_1)=H_n(\mu_1,t_1)/G_n(\mu_1,t_1)$. For saving the computation time, we can set an upper limit $\bar{n}$ for n. That is, if $G_n(\mu_1,t_1)=0$ for all $n=1,\cdots,\bar{n}$, we then stop the seeking at the updating time t_1 and consider ℓ belongs to the original set $\{\ell\in\mathbb{R}:\underline{D}\le\ell\le\overline{D}\}$ which leads to the output of the identifier is equal to the estimate at the last time instant, i.e., $\hat{D}(t_1)=\hat{D}(t_0)$, according to (60). The same computation process is followed for the subsequent updating time instants $t_2,t_3,\ldots$. For many practical applications, such as simulating a deep-sea construction vessel, locating non-zero values of $G_n(\mu_{i+1},t_{i+1})$ is a straightforward task following the algorithm described above.

Please note that even though the actuator states $v(x,t)$ are measurable in this full-state feedback case, for the delay estimation, one cannot adopt the "naive" method–that is, taking the time and spatial derivatives of the signal $v(x,t)$ to calculate d in (10) straightforwardly– because of the following two reasons: 1) taking the time derivative of the measured signals always leads to the undesired noise amplification in practice; 2) the possible zero values of $v_t(x,t)$ accompanied with the unknown delay D will engender singularity.

C. Delay-adaptive controller

With the sequence of time instants $\{t_i\ge 0\}_{i=0}^{\infty}$, $i\in\mathbb{Z}^+$ determined by the triggering mechanism (48), and the parameter identifier (60), the delay-compensated adaptive control algorithm $U_{\mathrm{d}}(t)$ on $t\in[t_i,t_{i+1})$ is designed as

$$U_{\mathrm{d}}(t) = \begin{cases} r\left(\sin(\omega(t-t_i+\dfrac{\pi}{2\omega}))-1\right), \\ if\ t_i>T_{\mathrm{f}}-2T\ and\ t_{i-1}\le T_{\mathrm{f}}-2T\ and\ i\ge 1 \\ \ and\ U_{\mathrm{d}}(t)\equiv 0\ on\ t\in[0,t_i) & (61a) \\ \int_0^1 M_1(y;\hat{D}(t_i))z(y,t)dy + \int_0^1 M_2(y;\hat{D}(t_i))w(y,t)dy \\ +\int_0^1 M_3(y;\hat{D}(t_i))v(y,t)dy \\ +M_4(\hat{D}(t_i))X(t),\quad otherwise & (61b) \end{cases}$$

where $T_{\mathrm{f}}-2T\ge 0$ according to (49). The equation (61b) is the result of replacing the unknown delay D in the nominal continuous-in-time feedback (33) with the estimate $\hat{D}(t_i)$ that is generated with the triggered batch least-squares identifier (60). Defining the time instant t_i satisfying the condition in (61a) as t_z, (61a) is an excitation implemented in a time interval $[t_z,t_{z+1})$ once U_d identically zero on $[0,t_z)$ is detected, to avoid the case that $U_{\mathrm{d}}(t)$ is identically zero on $t\in[0,t_{z+1})$, whose purpose is to ensure the exact identification of the unknown delay in the prescribed time T_{f}, which will be clear in the proof of Lemma 5. The nonzero constant r,ω in (61a) are free design parameters. Some guidelines about choosing the free design parameters r,ω,T_{f} from the practical point of view is given in Remark 2.

Remark 2 (Selections of free r,ω,T_{f} in practice): The constant r can be chosen small enough in practice to reduce the effect of the excitation (61a) on the control performance. The frequency ω in (61a) should be selected away from the natural inherent frequency of the plant to avoid the appearance of syntony. The prescribed identification time T_{f}, together with the maximum dwell time T, are positively related to the amount of the measurement data used in parameter estimation. The larger T_{f},T would improve the robustness to the sensor measurement error but prolong the time till exact parameter identification. On the contrary, the smaller T_{f},T contributes to the fast identification of the unknown delay, however, the robustness to the measurement error may be reduced. How to improve the robustness to the sensor measurement error under a short prescribed identification time T_{f},T is our future work.

Proposition 1 (Existence of solution in an interval): For every $(z[t_i],w[t_i],v[t_i])^T\in L^2((0,1);\mathbb{R}^3)$, $X(t_i)\in\mathbb{R}^m$, there exists a unique (weak) solution $((z,w,v)^T,X)\in C^0([t_i,t_{i+1}];L^2(0,1);\mathbb{R}^3)\times C^0([t_i,t_{i+1}];\mathbb{R}^m)$ to the system (1)–(4), (9)–(12), (61).

Proof: The proof is shown in Appendix C. ■

V. Main result

Before presenting the main theorem, we propose the following technical lemmas, where when we say that $v(x,t)$ is equal to zero for $x\in[0,1],t\in[\mu_{i+1},t_{i+1}]$, or not identically zero on the same domain, we mean except possibly for finitely many discontinuities of the functions $v(x,t)$. These discontinuities are isolated curves in the rectangle $[0,1]\times[\mu_{i+1},t_{i+1}]$.

Lemma 1 ($G_n(\mu_{i+1},t_{i+1})=0$): The sufficient and necessary condition of $G_n(\mu_{i+1},t_{i+1})=0$ for all $n\in\mathbb{N}$ is $v[t]=0$ on $t\in[\mu_{i+1},t_{i+1}]$.

Proof: Necessity: If $G_n(\mu_{i+1},t_{i+1})=0$ for all $n\in\mathbb{N}$, then the definition (59) in conjunction with continuity of $g_n(t)$ for $t\in[\mu_{i+1},t_{i+1}]$ (because of the definition (54) and the fact that $v\in C^0([t_i,t_{i+1}];L^2(0,1))$ in Proposition 1) implies

$$g_n(t)=0,\quad t\in[\mu_{i+1},t_{i+1}]. \tag{62}$$

According to the definition (54), the equation (62) implies

$$\int_0^1 \sin(x\pi n)v(x,t)dx=0,\quad t\in[\mu_{i+1},t_{i+1}] \tag{63}$$

for all $n\in\mathbb{N}$. Since the set $\{\sqrt{2}\sin(x\pi n): n=1,2,\ldots\}$ is an orthonormal basis of $L^2(0,1)$, we have $v[t]=0$ for $t\in[\mu_{i+1},t_{i+1}]$.

Sufficiency: If $v[t]=0$ on $t\in[\mu_{i+1},t_{i+1}]$, then $G_n(\mu_{i+1},t_{i+1})=0$ for all $n\in\mathbb{N}$ is obtained directly by recalling (59) and (54). ■

Lemma 2 (The identifier properties at t_{i+1}): For the adaptive estimates defined by (60), the following statements hold:

- If $v[t]$ is not identically zero for $t\in[\mu_{i+1},t_{i+1}]$, then $\hat{D}(t_{i+1})=D$.
- If $v[t]$ is identically zero for $t\in[\mu_{i+1},t_{i+1}]$, then $\hat{D}(t_{i+1})=\hat{D}(t_i)$.

Proof: Define a set

$$S_i=\Big\{\underline{D}\le\ell\le\overline{D}:\ H_n(\mu_{i+1},t_{i+1})=G_n(\mu_{i+1},t_{i+1})\ell,\quad n=1,2,\cdots\Big\}. \tag{64}$$

From (57), we know that $D\in S_i$. If S_i is a singleton, it is nothing else but the generated adaptive estimate $\hat{D}(t_{i+1})$ by (60), which is equal to the true delay D.

1) If $v[t]$ is not identically zero for $t\in[\mu_{i+1},t_{i+1}]$, recalling Lemma 1, there exists $n\in\mathbb{N}$ such that $G_n(\mu_{i+1},t_{i+1})\neq0$. Now defining the index set I as the set of all $n\in\mathbb{N}$ with $G_n(\mu_{i+1},t_{i+1})\neq0$, then (64) implies that

$$S_i=\left\{\ell=\frac{H_n(\mu_{i+1},t_{i+1})}{G_n(\mu_{i+1},t_{i+1})},n\in I\right\}$$

is a singleton, and therefore from (60) we get $\hat{D}(t_{i+1})=D$.

2) If $v[t]$ is identically zero on $t\in[\mu_{i+1},t_{i+1}]$, according to (53), (54), (58), (59), one obtains

$$G_n(\mu_{i+1},t_{i+1})=H_n(\mu_{i+1},t_{i+1})=0,\quad n\in\mathbb{N},$$

and it follows that $S_i=\{\underline{D}\le\ell\le\overline{D}\}$. Then, from (60) one arrive at $\hat{D}(t_{i+1})=\hat{D}(t_i)$.

The proof is complete. ■

Lemma 3 (The identifier properties for $t\in[t_i,\lim_{k\to\infty}(t_k))$): If $\hat{D}(t_i)=D$ for certain $i\in\mathbb{Z}^+$, then $\hat{D}(t)=D$ for all $t\in[t_i,\lim_{k\to\infty}(t_k))$.

Proof: According to Lemma 2, we have that $\hat{D}(t_{i+1})$ is equal to either D or $\hat{D}(t_i)$. Therefore, if $\hat{D}(t_i)=D$, then $\hat{D}(t_{i+1})=D$. Repeating this process, we then have $\hat{D}(t)=D$ for all $t\in[t_i,\lim_{k\to\infty}(t_k))$. The proof is complete. ■

Lemma 4 (Existence of a minimum dwell-time): There exists a positive constant τ_d such that $t_{i+1}-t_i\ge\tau_d$ for all $i\in\mathbb{Z}^+$.

Proof: The result is established by discussing the following two cases:

- Case 1: The exact identification has not been achieved for $t\in[0,t_i]$. According to Lemmas 2 and 3, we know $\hat{D}(t)\equiv\hat{D}(0)$ on $t\in[0,t_{i+1})$. Recalling Proposition 1, we obtain that $\Omega(t)$ is continuous on $t\in[t_i,t_{i+1})$, with possible finite non-differentiable points (though it is differentiable from the left and from the right, i.e. the left and right derivatives are finite, at those points). Denoting the maximum rate of change of $\Omega(t)$ on $t\in(t_i,t_{i+1})$ as V_i, that is, $V_i=\max\{\max_{t\in(t_i,t_{i+1})/I_i}|\dot{\Omega}(t)|,A_i\}$ where I_i is the set of those possible finite non-differentiable points, and where the set A_i is the absolute values of left and right derivatives at the points in I_i. Recalling the triggering mechanism (48), the lower bound $\underline{\tau}_i$ of the dwell time is given by

$$\underline{\tau}_i=\begin{cases}\min\left\{\frac{((1+a)\hat{\Upsilon}(\hat{D}(0))-1)\Omega(t_i)}{V_i},T\right\}>0, & \text{if } \Omega(t_i)\neq0\\ T, & \text{if } \Omega(t_i)=0.\end{cases} \tag{65}$$

- Case 2: The exact identification has been achieved for $[0,t_i]$. In this case, we have $t_{i+1}-t_i=T$. We prove this as follows. Once the exact delay identification is achieved, the delay-adaptive control input is identical to the nominal delay-compensated control input in Section III. When $\Omega(t_i)\neq0$, we have that $\Omega(t)\le\Upsilon\Omega(t_i)$ for $t_i\le t\le t_{i+1}$ according to Theorem 1. It follows from $\hat{\Upsilon}(\hat{D}(t_i))=\hat{\Upsilon}(D)=\Upsilon$ that $\Omega(t)<(1+a)\hat{\Upsilon}(\hat{D}(t_i))\Omega(t_i)$ for $t_i\le t\le t_{i+1}$. Thus $t_{i+1}-t_i=T$ according to (48). When $\Omega(t_i)=0$, we straightforwardly have $t_{i+1}-t_i=T$ according to the second equation in (48) and therefore, $t_{i+1}-t_i=T$.

The lemma is thus obtained. ■

Corollary 1 (Well-posedness of the closed-loop system): No Zeno phenomenon occurs, i.e., $\lim_{i\to\infty}t_i=+\infty$, and the closed-loop system is well-posed in the sense that for every $(z[0],w[0])^T\in L^2((0,1);\mathbb{R}^2)$, $X(0)\in\mathbb{R}^m$, and $\hat{D}(0)\in[\underline{D},\overline{D}]$, there exists a unique (weak) solution $((z,w,v)^T,X)\in C^0(\mathbb{R}_+;L^2(0,1);\mathbb{R}^3)\times C^0(\mathbb{R}_+;\mathbb{R}^m)$, and $\hat{D}(t)\in\{\ell\in\mathbb{R}:\underline{D}\le\ell\le\overline{D}\}$ for $t\in[0,\infty)$, to the system consisting of (1)–(4), (9)–(12), (60), and (61).

Proof: Recalling Lemma 4, we have that

$$t_i\ge\tau_d i,\quad i\in\mathbb{Z}^+,$$

where $\tau_d>0$, that is,

$$\lim_{i\to\infty}(t_i)=+\infty, \tag{66}$$

which implies a solution defined on $\mathbb{R}_+$ in the subsequent analysis.

From the initial data $(z[0],w[0])^T\in L^2((0,1);\mathbb{R}^2)$, $X(0)\in\mathbb{R}^m$ and (12), recalling the result in Proposition 1 for $i=0$, it follows that $((z,w,v)^T,X)\in$

$C^0([t_0,t_1];L^2(0,1);\mathbb{R}^3) \times C^0([t_0,t_1];\mathbb{R}^m)$, which implies $(z[t_1],w[t_1],v[t_1])^T \in L^2((0,1);\mathbb{R}^3)$, $X(t_1) \in \mathbb{R}^m$. Recalling the result in Proposition 1 for $i=1$, together with the solution obtained for $[t_0,t_1]$, we have that $((z,w,v)^T,X) \in C^0([t_0,t_2];L^2(0,1);\mathbb{R}^3) \times C^0([t_0,t_2];\mathbb{R}^m)$. Repeating the above steps, we obtain that $((z,w,v)^T,X) \in C^0([t_0,t_i];L^2(0,1);\mathbb{R}^3) \times C^0([t_0,t_i];\mathbb{R}^m)$ for $i \in \mathbb{N}$. Applying (66), we thus have $((z,w,v)^T,X) \in C^0([\mathbb{R}_+;L^2(0,1);\mathbb{R}^3) \times C^0(\mathbb{R}_+;\mathbb{R}^m)$. It is straightforwardly obtained from (60) that $\hat{D}(t) \in [\underline{D},\overline{D}]$ if $\hat{D}(0) \in [\underline{D},\overline{D}]$.

Corollary 1 is thus obtained. ∎

Lemma 5 (Finite-time convergence of the update law): The estimate $\hat{D}$ converges to the true value no latter than T_f, i.e.,

$$\hat{D}(t) = D,\ \forall t \in [t_f,\infty) \tag{67}$$

where $0 < t_f \leq T_\mathrm{f}$.

Proof: According to (61), we conclude that the control input $U_\mathrm{d}(t)$ is not identically zero on $t \in [0,t_{z+1})$ where the time instant t_i satisfying the condition in (61a) is denoted as t_z. There exists a time instant $t_f \leq t_{z+1}$ $(f>0)$ such that $U_\mathrm{d}(t)$ is not identically zero on $t \in [\mu_f,t_f]$. Recalling (10), (11) where $U(t)$ has been replaced by $U_\mathrm{d}(t)$, we conclude that the actuator state $v[t]$ is not identically zero on $t \in [\mu_f,t_f]$. Recalling Lemma 2, Lemma 3, and Corollary 1, we thus obtain (67). According to (61a), (48), we have

$$t_z < t_{z+1} \leq T_\mathrm{f}. \tag{68}$$

Recalling $t_f \leq t_{z+1}$, this lemma is obtained. ∎

Now, we are in a position to state our main result in the following theorem, i.e., exponential regulation of the plant and actuator states.

Theorem 2: For all initial data $(z[0],w[0])^T \in L^2(0,1)$, $X(0) \in \mathbb{R}^m$, $\hat{D}(0) \in [\underline{D},\overline{D}]$, considering the closed-loop system consisting of the plant (1)–(4), (9)–(12), the controller (61), the triggering mechanism (48), and the least-squares identifier (60), the exponential regulation of the closed-loop system is obtained in the sense that there exist positive constants M,λ_1 such that

$$\Omega(t) \leq Me^{-\lambda_1 t},\quad t \geq 0, \tag{69}$$

where $\Omega(t)$ is defined in (35).

Proof: Case 1: (61a) is not executed. Then the delay-adaptive control law U_d is (61b) all the time. Replacing the nominal control law U by U_d defined by (61b) in (11), through the transformations in Section III, the right boundary condition of the actuator PDE (30) in the target system (17)–(20), (28)–(30) becomes

$$\hat{u}(0,t) = \xi(t), \tag{70}$$

where

$$\begin{aligned}\xi(t) =& U_\mathrm{d}(t;\hat{D}) - U(t;D)\\ =& \int_0^1 (M_1(y;\hat{D}) - M_1(y;D))z(y,t)dy\\ &+ \int_0^1 (M_2(y;\hat{D}) - M_2(y;D))w(y,t)dy\\ &+ \int_0^1 (M_3(y;\hat{D}) - M_3(y;D))v(y,t)dy\\ &+ (M_4(\hat{D}) - M_4(D))X(t).\end{aligned} \tag{71}$$

Taking the derivative of (36) along the target system states corresponding to the even-based closed-loop system consisting of (17)–(20), (28), (29), and (70), through a similar process in (44), recalling conditions (37)–(40) on δ, r_a, r_c, and r_d (we emphasize that conditions (37)–(40) only depend on the known plant parameters and the known bounds of the unknown parameters in Assumption 3), we obtain

$$\dot{V}(t) \leq -\lambda_1 V(t) + \frac{r_c}{2D}\xi(t)^2,\quad t \geq 0, \tag{72}$$

where λ_1 is given in (46). According to (67) and (71), one can establish that

$$\xi(t) \equiv 0,\quad t \in [t_f,\infty). \tag{73}$$

We then have that

$$\dot{V}(t) \leq -\lambda_1 V(t),\quad t \geq t_f. \tag{74}$$

Multiplying both sides of (74) by $e^{\lambda_1 t}$ and integrating the resulting terms from t_f to t lead to the following inequality

$$V(t) \leq V(t_f)e^{-\lambda_1(t-t_f)},\quad t \geq t_f,$$

which, by virtue of (41), is equivalent to

$$\Omega(t) \leq \Upsilon\Omega(t_f)e^{-\lambda_1(t-t_f)},\quad t \geq t_f, \tag{75}$$

where Ω is defined in (35) and the positive constant Υ is given in (47).

Note that the norm estimate (75) is only true for $t \geq t_f$. Next, we extend our analysis for $t \in [0,t_f]$. With the help of (41), (71), we obtain from (72) that

$$\dot{V}(t) \leq -\lambda_1 V(t) + Q(\hat{D}(0))V(t),\quad t \in [0,t_f), \tag{76}$$

where the positive constant $Q(\hat{D}(0))$ is

$$\begin{aligned}Q(\hat{D}(0)) = \max_{y\in[0,1]} \Big\{ &(K_1(0,y;\hat{D}(0)) - K_1(0,y;D))^2,\\ &(K_2(0,y;\hat{D}(0)) - K_2(0,y;D))^2, (R(0,y;\hat{D}(0)) - R(0,y;D))^2,\\ &(\eta(0;\hat{D}(0)) - \eta(0;D))^2 \Big\} \frac{2r_c}{D\xi_1\xi_3}\end{aligned} \tag{77}$$

which is derived by finding an upper bound for $\xi(t)^2$ (71) in the form of target states $\beta,\alpha,\hat{u},X$, and recalling (41).

Hence, the following holds

$$\Omega(t) \leq \Upsilon\Omega(0)e^{\lambda_2(\hat{D}(0))t},\quad t \in [0,t_f], \tag{78}$$

where

$$\lambda_2(\hat{D}(0)) = |Q(\hat{D}(0)) - \lambda_1| > 0,$$

and the positive constant Υ is given in (47). Therefore, it straightforwardly follows that

$$\Omega(t_f) \leq \Upsilon e^{\lambda_2(\hat{D}(0))t_f}\Omega(0). \tag{79}$$

Considering (78), combining (75) and (79) yields

$$\Omega(t) \leq \Upsilon^2 e^{(\lambda_2(\hat{D}(0))+\lambda_1)t_f}\Omega(0)e^{-\lambda_1 t},\quad t \geq 0, \tag{80}$$

which is equivalent to (69) with

$$M=\Upsilon^2 e^{(\lambda_2(\hat{D}(0))+\lambda_1)t_f}\Omega(0).$$

Case 2: (61a) is executed. Denoting the time instant t_i satisfying the condition in (61a) as t_z, we know from (61) that

$$U_{\rm d}=\begin{cases}0, & t\in[0,t_z) \quad (81a)\\ r\left(\sin(\omega(t-t_i+\frac{\pi}{2\omega}))-1\right), & t\in[t_z,t_{z+1}) \quad (81b)\\ U(t;D), & t\in[t_{z+1},\infty) \quad (81c)\end{cases}$$

and $t_f=t_{z+1}$ in Lemma 5, recalling Lemmas 2 and 3 as well as (10), (11) where $U(t)$ has been replaced by $U_{\rm d}(t)$.

Therefore, following (73)–(75), applying (81c) that implies that ξ in (71) is identically zero on $t\ge t_{z+1}$, we have

$$\Omega(t)\le\Upsilon\Omega(t_{z+1})e^{-\lambda_1(t-t_{z+1})},\quad t\ge t_{z+1}. \tag{82}$$

Following (76)–(79), recalling (81a), we have

$$\Omega(t)\le\Upsilon\Omega(0)e^{\lambda_3 t},\quad t\in[0,t_z], \tag{83}$$

for $t\in[0,t_z)$, where $\lambda_3=Q_1-\lambda_1$ and the positive constant Q_1 is the one in (77) removing $K_1(0,y;\hat{D}(0))$, $K_2(0,y;\hat{D}(0))$, $R(0,y;\hat{D}(0))$, $\eta(0;\hat{D}(0))$. This implies

$$\Omega(t_z)\le\Upsilon\Omega(0)e^{|\lambda_3|t_z}. \tag{84}$$

Similarly, we obtain from (81b) that

$$\Omega(t)\le\Upsilon\Omega(t_z)e^{\lambda_4(t-t_z)}+\frac{4r_cr^2(e^{\lambda_4(t-t_z)}-1)}{\lambda_4 D\xi_1\xi_3},\quad t\in[t_z,t_{z+1}],$$

where $\lambda_4=2Q_1-\lambda_1$. Applying (68) and (84), we have

$$\Omega(t_{z+1})\le\Upsilon^2\Omega(0)e^{|\lambda_3|T_{\rm f}+|\lambda_4|T}+\frac{4r_cr^2(e^{|\lambda_4|T}-1)}{|\lambda_4|D\xi_1\xi_3}. \tag{85}$$

Inserting (85) into (82), one obtains (69) where

$$M=\Upsilon^3\Omega(0)e^{|\lambda_3|T_{\rm f}+|\lambda_4|T+\lambda_1T_{\rm f}}+\frac{4\Upsilon r_c(e^{|\lambda_4|T}-1)e^{\lambda_1T_{\rm f}}}{|\lambda_4|D\xi_1\xi_3}r^2. \tag{86}$$

The proof of the theorem is complete. ■

VI. Simulation

A deep-sea construction vessel (DCV) is used to place equipment to be installed at the predetermined location on the seafloor, which is shown in Figure 2. Different from [57] that deals with a known sensor delay that exists in the large-distance transmission of the sensing signal from the seafloor to the vessel on the ocean surface through a set of acoustics devices, we consider all possible delays here (including the transmission of the sensing signal, computation of the control law, and the delay in the hydraulic actuator for the ship-mounted crane and so on) as an unknown delay in the control input channel. By designing a control input at the top of the crane cable, our goal is to reduce the oscillations of the crane cable with the purpose of placing the payload attached at the bottom of the cable in the target area, despite the presence of the unknown delay.

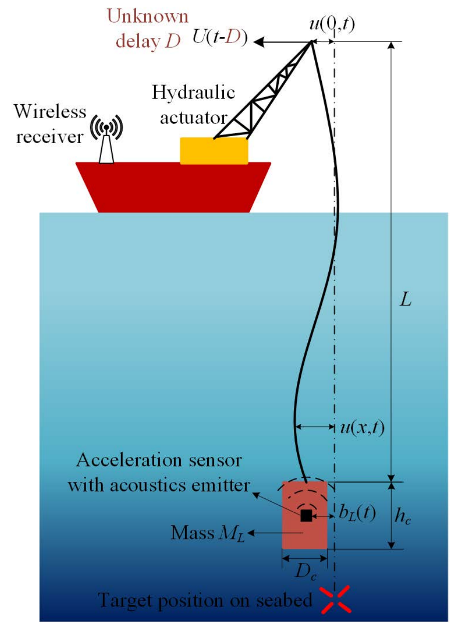

Fig. 2: Deep-sea construction vessel.

A. Model

The following dynamic model of cable-payload lateral oscillations in DCV is taken from [57],

$$T_0u_{\bar{x}}(0,t)=U(t-D), \tag{87}$$
$$\rho u_{tt}(\bar{x},t)=T_0u_{\bar{x}\bar{x}}(\bar{x},t)-d_cu_t(\bar{x},t), \tag{88}$$
$$u(L,t)=b_L(t), \tag{89}$$
$$M_L\ddot{b}_L(t)=-d_L\dot{b}_L(t)+T_0u_{\bar{x}}(L,t), \tag{90}$$

$\forall(\bar{x},t)\in[0,L]\times[0,\infty)$. The state $u(\bar{x},t)$ describes the lateral oscillation displacement along the cable, and $b_L(t)$ denotes that of the payload. The control input U is subject to the unknown time delay D mentioned above. The static tension T_0 is defined as $T_0=M_Lg-F_{\rm buoyant}$, where the buoyancy $F_{\rm buoyant}$ is $F_{\rm buoyant}=\frac{1}{4}\pi D_c^2h_c\rho_sg$. The physical parameters of the deep-sea construction vessel are shown in Table I.

Like [57], after applying the Riemann transformations

$$z(\bar{x},t)=u_t(\bar{x},t)-\sqrt{\frac{T_0}{\rho}}u_{\bar{x}}(\bar{x},t), \tag{91}$$

$$w(\bar{x},t)=u_t(\bar{x},t)+\sqrt{\frac{T_0}{\rho}}u_{\bar{x}}(\bar{x},t), \tag{92}$$

introducing a space normalization variable

$$x=\frac{\bar{x}}{L}\in[0,1], \tag{93}$$

and defining $X(t)=\dot{b}_L(t)$, equations (87)–(90) are rewritten as the considered plant (1)–(5) with the coefficients

$$c_0=2\sqrt{\frac{1}{T_0\rho}},\quad q_1=q_2=\frac{1}{L}\sqrt{\frac{T_0}{\rho}}, \tag{94}$$

$$d_1=d_2=d_3=d_4=\frac{-d_c}{2\rho}, q=-1,\ p=1, \tag{95}$$

This article has been accepted for publication in IEEE Transactions on Automatic Control. This is the author's version which has not been fully edited and content may change prior to final publication. Citation information: DOI 10.1109/TAC.2024.3399629

TABLE I: Physical parameters of the DCV.

Parameters (units)	values
Cable length L (m)	1500
Cable linear density ρ (kg/m)	7.5
Payload mass M_L (kg)	3.5×10^5
Gravitational acceleration g (m/s^2)	9.8
Cable material damping coefficient d_c (N·s/m)	0.8
Height of payload modeled as a cylinder h_c (m)	7.5
Diameter of payload modeled as a cylinder D_c (m)	5
Damping coefficient at payload d_L (N·s/m)	1.2×10^5
Seawater density ρ_s (kgm^{-3})	1024

$$C=2,\ A=\frac{-d_L}{M_L}+\frac{\sqrt{T_0\rho}}{M_L},\ B=-\frac{\sqrt{T_0\rho}}{M_L}, \tag{96}$$

which is the simulation model in this section, where it can be checked that the plan parameters in (94)–(96) satisfy Assumptions 1, 2 by recalling Table I.

The initial conditions are defined as

$$z(x,0)=8\sin(5\pi x(1-x)),\quad w(x,0)=-8\cos(5\pi x),$$

thereby, $X(0)=1.13$, recalling (4), which physically corresponds to the initial oscillation velocities of the payload. The unknown delay D is set as 1, and the known bounds $\underline{D}$ and $\overline{D}$ are assumed as 0.01 and 2. We will show the simulation results of the following four cases:

- Open loop: the control input is zero;
- Nonadaptive control: the nominal delay-compensated control with the unknown delay D replaced by its estimate 0.25;
- Delay-adaptive control with the initial delay estimate $\hat{D}(0)=0.25$, where the design parameter K in (22) is chosen as $K=-18$;
- Delay-adaptive control with the initial delay estimate $\hat{D}(0)=1.5$, where the design parameter K in (22) is chosen as $K=-13$.

Other design parameters are

$$\delta=-0.36,\ r_a=1.02,\ r_c=1,r_d=0.02,\ a=2,$$
$$T=3.12,\ \tilde{N}=10,T=8,r=0.5,\omega=1$$

according to (37)–(40), where $a,T,\tilde{N},T$ are free but positive, and r,ω are free. Actually, like most physical systems, (61a) associated with r,ω has not been activated in the simulation because the control signal is not identically zero for a certain time period from the beginning. The parameter $\bar{n}$ mentioned in Remark 1 is set as $\bar{n}=2$.

Remark 3: In addition to Remark 1 about the implementation of the delay identifier, some more things are worth noting in the simulation. 1) Approximating the integration with respect to the space variable in the identifier as the summation operator will cause a tiny error between the final parameter estimate and the true value in the simulation result, which will be seen in Fig. 4. The smaller space step adopted in the simulation will make the error smaller. 2) The error of approximation in the simulation will also lead to tiny differences between the outputs of the identifer at each updating time even if the effective parameter deification has been achieved. Therefore, we set a small margin to tolerate the approximation error, that is–if the difference between the estimates from the identifier at two adjacent updating times is smaller than 2% of the true value, we consider that this difference is caused by the approximation error in the simulation, and thus keep the estimate value as same as the one at the former updating time.

B. Simulation result

The numerical computation is conducted using the finite difference method with the step sizes of t and x as 0.001, and 0.02, respectively. The approximate solutions of the kernel PDEs used in the control law, which is defined by (61), (48), (60) where the integral operators are approximated by sums, are also solved by the finite difference method based on the discretization of the triangular domain into a uniformly spaced grid with the interval of 0.02.

The designed delay-adaptive control input and the estimate of the unknown delay are shown in Figures 3 and 4, respectively, from which we know that the identification of the unknown delay is achieved at the first triggering time, no matter the initial delay estimate is less than ($\hat{D}(0)=0.25$) or larger than ($\hat{D}(0)=1.5$) the true value $D=1$. As mentioned in Remark 3, the tiny differences between the delay estimate and its true values come from the error of approximation—that is, approximating the integration with respect to the space variable from 0 to 1 in the identifier as the summation operator for the 51 spatial discrete points with the fixed interval of 0.02. The time evolution of the ODE state $X(t)$ is shown in Figure 5, where the brown dashed line, the red dashed line, the black solid line, and the blue dot-dash line show the results of the four cases mentioned in Section VI-A, respectively. Although both the nonadaptive delay-compensated controller and the delay-adaptive controllers can attenuate the state of the ODE in comparison to the open loop scenario, Figure 5 further reveals the "delay mismatch" in the non-adaptive control law leads to slower convergence after the time point when the exact delay estimate is obtained and the updated input signal reaches the ODE through the transport PDEs. Even though the simulation model, like many practical models that usually include damping, is not an open-loop unstable plant, the proposed control design still shows improved convergence rates under the proposed delay-adaptive controllers as compared to both the open-loop case and nonadaptive delay-compensated controller. Similarly, it is shown in Figures 6, 7, and 8 that the PDE plant states $z(x,t)$, $w(x,t)$ and the actuator state $v(x,t)$ all converge to zero when the system is subject to the proposed delay-adaptive control inputs with $\hat{D}(0)=0.25$ or $\hat{D}(0)=1.5$.

It is easy to obtain the oscillation energy of the cable in DCV $\frac{\rho}{2}\|u_t(\cdot,t)\|^2+\frac{T_0}{2}\|u_x(\cdot,t)\|^2=\frac{\rho}{8}\|w(\cdot,t)+z(\cdot,t)\|^2+\frac{\rho}{8}\|w(\cdot,t)-z(\cdot,t)\|^2$ by recalling (91)–(93). Therefore, it is known from the results $z(x,t)$ and $w(x,t)$ in Figures 6 and 7 that the oscillation energy of the cable decreases to zero fast under the proposed delay-adaptive controller. One can also observe from Figure 5 that the regulation performance of the ODE, i.e., the payload, is satisfied.

VII. Conclusion and Future Work

In this paper, we have proposed a delay-adaptive control scheme for a 2×2 hyperbolic PDE-ODE system, where the

This article has been accepted for publication in IEEE Transactions on Automatic Control. This is the author's version which has not been fully edited and content may change prior to final publication. Citation information: DOI 10.1109/TAC.2024.3399629

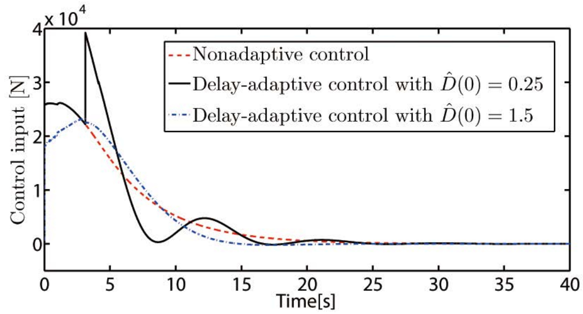

Fig. 3: The delay-adaptive control input $U_{\mathrm{d}}(t)$ with $\hat{D}(0) = 0.25$ or $\hat{D}(0) = 1.5$ and the nonadaptive control input $U_0(t)$.

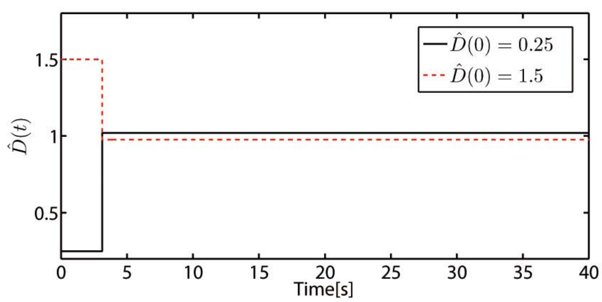

Fig. 4: Estimate of the unknown delay D under the initial estimate $\hat{D}(0) = 0.25$ or $\hat{D}(0) = 1.5$.

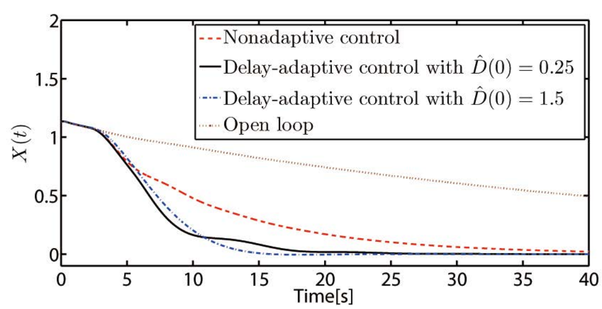

Fig. 5: The evolution of $X(t)$ under the delay-adaptive control $U_{\mathrm{d}}(t)$ with $\hat{D}(0) = 0.25$ or $\hat{D}(0) = 1.5$ and the nonadaptive control $U_0(t)$.

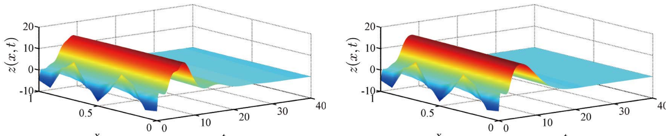

(a) $\hat{D}(0) = 0.25$ (b) $\hat{D}(0) = 1.5$

Fig. 6: The evolution of the plant state $z(x,t)$ under the delay-adaptive control $U_{\mathrm{d}}(t)$ with $\hat{D}(0) = 0.25$ or $\hat{D}(0) = 1.5$.

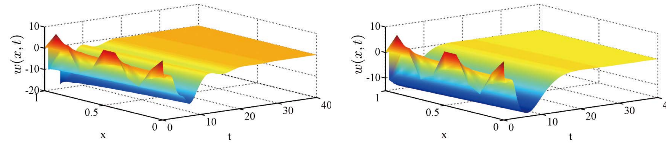

(a) $\hat{D}(0) = 0.25$ (b) $\hat{D}(0) = 1.5$

Fig. 7: The evolution of the plant state $w(x,t)$ under the delay-adaptive control $U_{\mathrm{d}}(t)$ with $\hat{D}(0) = 0.25$ or $\hat{D}(0) = 1.5$.

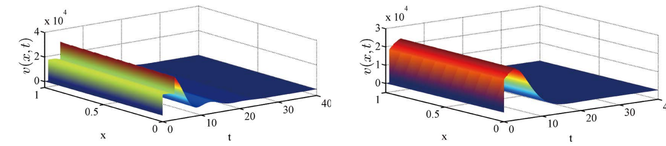

(a) $\hat{D}(0) = 0.25$ (b) $\hat{D}(0) = 1.5$

Fig. 8: The evolution of the actuator state $v(x,t)$ under the delay-adaptive control $U_{\mathrm{d}}(t)$ with $\hat{D}(0) = 0.25$ or $\hat{D}(0) = 1.5$.

input delay is arbitrarily large and unknown. The controller consists of a nominal delay-compensated control law, a batch least-squares identifier for the unknown delay, and a triggering mechanism to determine the update times of the identifier. We have proved that the proposed control guarantees: 1) the avoidance of Zeno phenomenon; 2) the identification of the unknown boundary input delay before the prescribed time; 3) the exponential regulation of both the plant and the actuator states to zero. The effectiveness of the proposed design is verified by numerical simulation in the control application of a deep-sea construction vessel subject to input delay. This paper only deals with the state-feedback adaptive-delay control design for coupled hyperbolic PDEs whose actuator states and plant states are measurable.

In our future work, the output-feedback control design with unmeasurable actuator and plant states, and improvement of the robustness to the sensor measurement error under a short expected identification time, will be considered.

VIII. Appendix

A. *Gain kernels PDEs and their associated boundary conditions*

(a) First-step transformation

The backstepping transformation (13) and (14) lead to the following PDE-ODE system of kernel conditions for $\varphi, \phi, \Psi, \Phi, \gamma$ and λ. These conditions are derived by mapping the original plant to the first intermediate system.

$$q_2\varphi_y(x,y) - q_1\varphi_x(x,y) - (d_4 - d_1)\varphi(x,y) - d_2\phi(x,y) = 0, \tag{A.1}$$

$$q_1\phi_x(x,y) + q_1\phi_y(x,y) + d_3\varphi(x,y) = 0, \tag{A.2}$$

$$q_2\Psi_x(x,y) - q_1\Psi_y(x,y) + (d_4 - d_1)\Psi(x,y) - d_3\Phi(x,y) = 0, \tag{A.3}$$

$$q_2\Phi_x(x,y) + q_2\Phi_y(x,y) - d_2\Psi(x,y) = 0, \tag{A.4}$$

$$q_1\gamma'(x) + \gamma(x)(A - d_1 I_n) + q_1 C\phi(x,0) = 0, \tag{A.5}$$

$$q_2\lambda'(x)-\lambda(x)(A-d_4I_n)-q_1C\Psi(x,0)=0, \tag{A.6}$$

with the boundary conditions

$$\varphi(x,x)=\frac{d_2}{q_1+q_2}, \tag{A.7}$$
$$q_2\varphi(x,0)+q_1p\phi(x,0)=\gamma(x)B, \tag{A.8}$$
$$\Psi(x,x)=\frac{-d_3}{q_1+q_2}, \tag{A.9}$$
$$q_2\Phi(x,0)+q_1p\Psi(x,0)=\lambda(x)B, \tag{A.10}$$
$$\lambda(0)=K^T, \tag{A.11}$$
$$\gamma(0)=C-pK^T, \tag{A.12}$$

where I_n is an identity matrix with dimension n.

Similarly, the boundary conditions of the gain kernels associated with the inverse backstepping transformation (15), (16), namely, $\bar\varphi,\bar\phi,\bar\gamma,\bar\Psi,\bar\Phi$ and $\bar\lambda$ are given by

$$q_2\bar\Psi_x(x,y)-q_1\bar\Psi_y(x,y)+(d_4-d_1)\bar\Psi(x,y)+d_3\bar\phi(x,y)=0, \tag{A.13}$$
$$q_1\bar\phi_x(x,y)+q_1\bar\phi_y(x,y)-d_2\bar\Psi(x,y)=0, \tag{A.14}$$
$$q_2\bar\varphi_y(x,y)-q_1\bar\varphi_x(x,y)-(d_4-d_1)\bar\varphi(x,y)+d_2\bar\Phi(x,y)=0, \tag{A.15}$$
$$q_2\bar\Phi_y(x,y)+q_2\bar\Phi_x(x,y)+d_3\bar\varphi(x,y)=0, \tag{A.16}$$
$$q_1\bar\gamma'(x)-\bar\gamma(x)(A+BK^T+d_1I_n)-d_2\bar\lambda(x)=0, \tag{A.17}$$
$$q_2\bar\lambda'(x)+\bar\lambda(x)(A+BK^T+d_4I_n)+d_3\bar\gamma(x)=0, \tag{A.18}$$

with the boundary conditions

$$\bar\Psi(x,x)=-\frac{d_3}{q_1+q_2}, \tag{A.19}$$
$$q_1p\bar\phi(x,0)+q_2\bar\varphi(x,0)=\bar\gamma(x)B, \tag{A.20}$$
$$\bar\varphi(x,x)=\frac{d_2}{q_1+q_2}, \tag{A.21}$$
$$q_2\bar\Phi(x,0)+q_1p\bar\Psi(x,0)=\bar\lambda(x)B, \tag{A.22}$$
$$\bar\lambda(0)=-K^T, \tag{A.23}$$
$$\bar\gamma(0)=pK^T-C. \tag{A.24}$$

The set of equations (A.1)–(A.12) and (A.13)–(A.24) are well-known for coupled linear heterodirectional hyperbolic PDE-ODE systems, and their well-posedness has been proved in Theorem 4.1 of [43].

(b) Second-step transformation

The gain kernels K_1,K_2 and η are defined below:

$$dK_{1x}(x,y)+q_1K_{1y}(x,y)=-d_1K_1(x,y), \tag{A.25}$$
$$dK_{2x}(x,y)-q_2K_{2y}(x,y)=-d_4K_2(x,y), \tag{A.26}$$
$$d\eta'(x)A_{\mathrm{m}}^{-1}+\eta(x)=0, \tag{A.27}$$

with the boundary conditions

$$K_1(1,y)=\frac{1}{c_0}\bar\Psi(1,y)-\frac{1}{c_0}q\bar\phi(1,y), \tag{A.28}$$
$$K_2(1,y)=\frac{1}{c_0}\bar\Phi(1,y)-\frac{1}{c_0}q\bar\varphi(1,y), \tag{A.29}$$
$$K_1(x,1)=\frac{qq_2}{q_1}K_2(x,1), \tag{A.30}$$
$$q_1pK_1(x,0)+q_2K_2(x,0)=\eta(x)B, \tag{A.31}$$
$$\eta(1)=-\frac{1}{c_0}q\bar\gamma(1)+\frac{1}{c_0}\bar\lambda(1). \tag{A.32}$$

The proof of well-posedness of (A.25)–(A.32) is given in Lemma 2 in [7]. To derive conditions (A.25)–(A.32), one needs to consider (21) and (23). Hence, (24) holds straightforwardly under the conditions (A.28), (A.29), (A.32). Taking the time and spatial derivatives of (23), inserting the results into (25), recalling (17)–(20), (24), one obtains

$$\begin{aligned}
&u_t(x,t)+du_x(x,t)-q_2K_2(x,1)c_0u(1,t)\\
=&v_t(x,t)+\int_0^1K_1(x,y)\alpha_t(y,t)dy+\int_0^1K_2(x,y)\beta_t(y,t)dy\\
&+dv_x(x,t)+d\int_0^1K_{1x}(x,y)\alpha(y,t)dy\\
&+d\int_0^1K_{2x}(x,y)\beta(y,t)dy\\
&+\eta(x)\dot X(t)+d\eta'(x)X(t)-q_2K_2(x,1)c_0u(1,t)\\
=&v_t(x,t)-q_1\int_0^1K_1(x,y)\alpha_x(y,t)dy\\
&+d_1\int_0^1K_1(x,y)\alpha(y,t)dy\\
&+q_2\int_0^1K_2(x,y)\beta_x(y,t)dy+d_4\int_0^1K_2(x,y)\beta(y,t)dy\\
&+dv_x(x,t)+d\int_0^1K_{1x}(x,y)\alpha(y,t)dy\\
&+d\int_0^1K_{2x}(x,y)\beta(y,t)dy+\eta(x)(A_{\mathrm{m}}X(t)+B\beta(0,t))\\
&+d\eta'(x)X(t)-q_2K_2(x,1)c_0u(1,t)\\
=&(q_2K_2(x,1)q-q_1K_1(x,1))\,\alpha(1,t)\\
&+\int_0^x(q_1K_{1y}(x,y)+d_1K_1(x,y)+dK_{1x}(x,y))\,\alpha(y,t)dy\\
&-(q_2K_2(x,0)+q_1K_1(x,0)p-\eta(x)B)\,\beta(0,t)\\
&+\int_0^x(d_4K_2(x,y)-q_2K_{2y}(x,y)+dK_{2x}(x,y))\,\beta(y,t)dy\\
&+\big(\eta(x)A_{\mathrm{m}}+d\eta'(x)\big)X(t)=0.
\end{aligned} \tag{A.33}$$

The necessary and sufficient conditions for (A.33) to hold are given as (A.25)–(A.27), (A.30), (A.31).

(c) Third-step transformation

The derivation of the gain kernels PDE R and R^I is performed as follows. Substituting the time and spatial derivatives of (27) into (25) and recalling (28)–(30), we have

$$\begin{aligned}
&u_t(x,t)+du_x(x,t)-q_2K_2(x,1)c_0u(1,t)\\
=&\hat u_t(x,t)+\int_x^1R(x,y)\hat u_t(y,t)dy+d\hat u_x(x,t)\\
&+d\int_x^1R_x(x,y)\hat u(y,t)dy-dR(x,x)\hat u(x,t)\\
&-q_2K_2(x,1)c_0\hat u(1,t)\\
=&-d\int_x^1R(x,y)\hat u_x(y,t)dy+d\int_x^1R_x(x,y)\hat u(y,t)dy\\
&-dR(x,x)\hat u(x,t)-q_2K_2(x,1)c_0\hat u(1,t)\\
=&-(dR(x,1)+q_2K_2(x,1)c_0)\hat u(1,t)\\
&+d\int_x^1(R_x(x,y)+R_y(x,y))\hat u(y,t)dy=0.
\end{aligned} \tag{A.34}$$

For (A.34) to hold, the following equality must be satisfied:

$$R_x(x,y)+R_y(x,y)=0, \tag{A.35}$$
$$dR(x,1)=-q_2c_0K_2(x,1), \tag{A.36}$$

which obviously admits a unique solution

$$R(x,y)=-\frac{q_2c_0}{d}K_2(x-y+1,1).$$

Similarly, substituting the time and spatial derivatives of (32) into (29) and recalling (25), we have

$$\begin{aligned}
&\hat{u}_t(x,t)+d\hat{u}_x(x,t)\\
=&u_t(x,t)+\int_x^1 P(x,y)u_t(y,t)dy+du_x(x,t)\\
&+d\int_x^1 P_x(x,y)u(y,t)dy-dP(x,x)u(x,t)\\
=&q_2K_2(x,1)c_0u(1,t)-d\int_x^1 P(x,y)u_x(y,t)dy\\
&+\int_x^1 P(x,y)q_2K_2(y,1)c_0dyu(1,t)\\
&+d\int_x^1 P_x(x,y)u(y,t)dy-dP(x,x)u(x,t)\\
=&\big(q_2K_2(x,1)c_0-dP(x,1)\\
&+\int_x^1 P(x,y)q_2K_2(y,1)c_0dy\big)u(1,t)\\
&+d\int_x^1 (P_y(x,y)+P_x(x,y))u(y,t)dy=0.
\end{aligned}$$

The equation above suggests that the kernel function P in the inverse transformation (32) satisfies the following PDE with the corresponding boundary value:

$$P_y(x,y)-P_x(x,y)=0, \tag{A.37}$$
$$P(x,1)=\frac{q_2}{d}K_2(x,1)c_0+\frac{1}{d}\int_x^1 P(x,y)q_2K_2(y,1)c_0dy, \tag{A.38}$$

whose well-posedness can be obtained by the method of characteristics.

B. Expressions of the controller gain functions M_1, M_2, M_3, M_4

The functions M_1, M_2, M_3, and M_4 are given as follows,

$$\begin{aligned}
M_1(y)=&\int_0^1 R(0,s)K_1(s,y)ds-K_1(0,y)\\
&+\int_0^1 R(0,s_1)\int_{s_1}^1 P(s_1,s)K_1(s,y)dsds_1\\
&-\int_y^1\Big[\int_0^1 R(0,y)K_1(y,s)dy-K_1(0,s)\\
&+\int_0^1 R(0,s_1)\int_{s_1}^1 P(s_1,y)K_1(y,s)dyds_1\Big]\phi(s,y)ds\\
&-\int_y^1\Big[\int_0^1 R(0,y)K_2(y,s)dy-K_2(0,s)\\
&+\int_0^1 R(0,s_1)\int_{s_1}^1 P(s_1,y)K_2(y,s)dyds_1\Big]\Psi(s,y)ds,\\
M_2(y)=&-\int_y^1\Big[\int_0^1 R(0,y)K_1(y,s)dy-K_1(0,s)\\
&+\int_0^1 R(0,s_1)\int_{s_1}^1 P(s_1,y)K_1(y,s)dyds_1\Big]\varphi(s,y)ds\\
&+\int_0^1 R(0,s)K_2(s,y)ds-K_2(0,y)\\
&+\int_0^1 R(0,s_1)\int_{s_1}^1 P(s_1,s)K_2(s,y)dsds_1\\
&-\int_y^1\Big[\int_0^1 R(0,y)K_2(y,s)dy-K_2(0,s)\\
&+\int_0^1 R(0,s_1)\int_{s_1}^1 P(s_1,y)K_2(y,s)dyds_1\Big]\Phi(s,y)ds,\\
M_3(y)=&R(0,y)+\int_0^y R(0,s)P(s,y)ds,\\
M_4=&\int_0^1 R(0,y)\eta(y)dy-\eta(0)\\
&+\int_0^1 R(0,y)\int_y^1 P(y,s)\eta(s)dsdy\\
&-\int_0^1\Big[\int_0^1 R(0,s)K_2(s,y)ds-K_2(0,y)\\
&+\int_0^1 R(0,s_1)\int_{s_1}^1 P(s_1,s)K_2(s,y)dsds_1\Big]\lambda(y)dy\\
&-\int_0^1\Big[\int_0^1 R(0,s)K_1(s,y)ds-K_1(0,y)\\
&+\int_0^1 R(0,s_1)\int_{s_1}^1 P(s_1,s)K_1(s,y)dsds_1\Big]\gamma(y)dy,
\end{aligned}$$

where K_1,K_2,η,R,P are parameterized by the unknown delay $D=\frac{1}{d}$ according to the conditions defined in Appendix A.

C. Proof of Proposition 1

Case 1: With the delay-adaptive control input U_d (61b), applying the following transformations,

$$\alpha(x,t)=e^{\frac{d_1}{q_1}x}\bar{\alpha}(x,t) \tag{C.1}$$
$$\beta(x,t)=e^{-\frac{d_4}{q_2}x}\bar{\beta}(x,t) \tag{C.2}$$

the target system, i.e., equivalently closed-loop system, is written as

$$\dot{X}(t)=A_{\mathrm{m}}X(t)+B\bar{\beta}(0,t), \tag{C.3}$$
$$\bar{\alpha}(0,t)=-p\bar{\beta}(0,t), \tag{C.4}$$
$$\bar{\alpha}_t(x,t)=-q_1\bar{\alpha}_x(x,t), \tag{C.5}$$
$$\bar{\beta}_t(x,t)=q_2\bar{\beta}_x(x,t), \tag{C.6}$$
$$\bar{\beta}(1,t)=c_0e^{\frac{d_4}{q_2}}\hat{u}(1,t)+qe^{\frac{d_1}{q_1}+\frac{d_4}{q_2}}\bar{\alpha}(1,t), \tag{C.7}$$
$$\hat{u}_t(x,t)=-d\hat{u}_x(x,t), \tag{C.8}$$
$$\begin{aligned}\hat{u}(0,t)=&-\int_0^1 \mathscr{K}_{1i}(y)\bar{\alpha}(y,t)dy-\int_0^1 \mathscr{K}_{2i}(y)\bar{\beta}(y,t)dy\\&+\int_0^1 \mathscr{R}_i(y)\hat{u}(y,t)dy-\eta_iX(t)\end{aligned} \tag{C.9}$$

for $t\in[t_i,t_{i+1})$ where $\mathscr{K}_{1i}(y)=(K_1(0,y;\hat{D}(t_i))-K_1(0,y;D))e^{\frac{d_1}{q_1}y}$, $\mathscr{K}_{2i}(y)=(K_2(0,y;\hat{D}(t_i))-K_2(0,y;D))e^{-\frac{d_4}{q_2}y}$, $\mathscr{R}_i(y)=R(0,y;\hat{D}(t_i))-R(0,y;D)$, $\eta_i=\eta(0;\hat{D}(t_i))-\eta(0;D)$ considering (31).

Next, we prove the well-posedness of (C.3)–(C.9) by the method of characteristics following [16]. Considering a constant $0<\bar{T}_i<\min\{t_{i+1}-t_i,\frac{1}{q_1},\frac{1}{q_2},\frac{1}{d}\}$, by the method of characteristics, for $\varsigma\in[0,\bar{T}_i]$ we get

$$\bar{\beta}(x,t_i+\varsigma)=\begin{cases}\bar{\beta}(x+q_2\varsigma,t_i), & x<1-q_2\varsigma\\ c_0e^{\frac{d_4}{q_2}}\hat{u}(1-d(\varsigma-\frac{1-x}{q_2}),t_i) & \\ +qe^{\frac{d_1}{q_1}+\frac{d_4}{q_2}}\bar{\alpha}(1-q_1(\varsigma-\frac{1-x}{q_2}),t_i) & x\geq 1-q_2\varsigma\end{cases} \tag{C.10}$$

$$\bar{\alpha}(x,t_i+\varsigma)=\begin{cases}\bar{\alpha}(x-q_1\varsigma,t_i), & x>q_1\varsigma\\ -p\bar{\beta}(q_2(\varsigma-\frac{x}{q_1}),t_i) & x\leq q_1\varsigma\end{cases} \tag{C.11}$$

Integrating (C.3) and recalling (C.10), we have

$$X(t_i+\varsigma)=A_{\rm m}\int_{t_i}^{t_i+\varsigma}X(\tau)d\tau+\int_0^{\varsigma}B\bar{\beta}(q_2\tau,t_i)d\tau+X(t_i) \tag{C.12}$$

for $\varsigma\in[0,\bar{T}_i]$. According to (C.8), (C.9), we also obtain by the method of characteristics that

$$\hat{u}(x,t_i+\varsigma)=\hat{u}(x-d\varsigma,t_i),\quad x>d\varsigma \tag{C.13}$$

and the solution $\hat{u}(x,t_i+\varsigma)$ for $x\leq d\varsigma$ is given by

$$\begin{aligned}&\hat{u}(x,t_i+\varsigma)=\hat{u}(0,t_i+t^*)\\&=-\int_0^1\mathscr{K}_{1i}(y)\bar{\alpha}(y,t_i+t^*)dy-\int_0^1\mathscr{K}_{2i}(y)\bar{\beta}(y,t_i+t^*)dy\\&\quad+\int_0^1\mathscr{R}_i(y)\hat{u}(y,t_i+t^*)dy-\eta_iX(t_i+t^*)\\&=s(t_i+t^*)+\int_0^{dt^*}\mathscr{R}_i(y)\hat{u}(0,t_i+t^*-\frac{y}{d})dy,\ x\leq d\varsigma\end{aligned} \tag{C.14}$$

where $t^*=\varsigma-\frac{x}{d}\in[0,\varsigma]$, and where

$$\begin{aligned}s(t_i+t^*)=&-\int_0^1\mathscr{K}_{1i}(y)\bar{\alpha}(y,t_i+t^*)dy\\&-\int_0^1\mathscr{K}_{2i}(y)\bar{\beta}(y,t_i+t^*)dy\\&-\eta_iX(t_i+t^*)+\int_{dt^*}^1\mathscr{R}_i(y)\hat{u}(y-dt^*,t_i)dy.\end{aligned} \tag{C.15}$$

Applying (C.10)–(C.12), one obtains

$$\begin{aligned}s(t_i+t^*)=&\int_0^{q_1t^*}\mathscr{K}_{1i}(y)(p\bar{\beta}(q_2(t^*-\frac{y}{q_1}),t_i))dy\\&-\int_{q_1t^*}^1\mathscr{K}_{1i}(y)\bar{\alpha}(y-q_1t^*,t_i)dy\\&-\int_0^{1-q_2t^*}\mathscr{K}_{2i}(y)\bar{\beta}(y+q_2t^*,t_i)dy\\&-\int_{1-q_2t^*}^1\mathscr{K}_{2i}(y)\left(c_0e^{\frac{d_4}{q_2}}\hat{u}(1-d(t^*-\frac{1-y}{q_2}),t_i)\right.\\&\left.+qe^{\frac{d_1}{q_1}+\frac{d_4}{q_2}}\bar{\alpha}(1-q_1(t^*-\frac{1-y}{q_2}),t_i)\right)dy\\&-\eta_i\left(A_{\rm m}\int_{t_i}^{t_i+t^*}X(\tau)d\tau+\int_0^{t^*}B\bar{\beta}(q_2\tau,t_i)d\tau+X(t_i)\right)\\&+\int_{dt^*}^1\mathscr{R}_i(y)\hat{u}(y-dt^*,t_i)dy.\end{aligned} \tag{C.16}$$

Recalling $(\bar{\alpha}[t_i],\bar{\beta}[t_i],\hat{u}[t_i])^T\in L^2((0,1);\mathbb{R}^3)$, $X(t_i)\in\mathbb{R}^m$ ensured by the initial condition $(z[t_i],w[t_i],v[t_i])^T\in L^2((0,1);\mathbb{R}^3)$, $X(t_i)\in\mathbb{R}^m$ and the transformations (13), (14), (23), (32), (C.1), (C.2), it is obtained from (C.16) that $s(t_i+t^*)$ is well-defined.

Defining $\rho=t^*-\frac{y}{d}$, we obtain from (C.14) that

$$\hat{u}(0,t_i+t^*)=s(t_i+t^*)+d\int_0^{t^*}\mathscr{R}_i(d(t^*-\rho))\hat{u}(0,t_i+\rho)d\rho, \tag{C.17}$$

for $t^*\in[0,\varsigma]$. Since $s(t_i+t^*)$ and $\mathscr{R}_i(d(t^*-\rho))$ are well defined for $t^*\in[0,\varsigma]$, where $\varsigma\in[0,\bar{T}_i]$, and in addition $\mathscr{R}_i(d(t^*-\rho))$ is also continuous in the interval, then (C.17) is a linear Volterra integral equation with a unique solution (see Theorem 5 in [29]). Recalling (C.10)–(C.14) and $(\bar{\alpha}[t_i],\bar{\beta}[t_i],\hat{u}[t_i])^T\in L^2((0,1);\mathbb{R}^3)$, $X(t_i)\in\mathbb{R}^m$, we obtain the well-posedness result in the sense of $((\bar{\alpha},\bar{\beta},\hat{u})^T,X)\in C^0([t_i,\bar{T}_i];L^2(0,1);\mathbb{R}^3)\times C^0([t_i,\bar{T}_i];\mathbb{R}^m)$. Then starting from $(\bar{\alpha}[\bar{T}_i],\bar{\beta}[\bar{T}_i],\hat{u}[\bar{T}_i])^T\in L^2((0,1);\mathbb{R}^3)$, $X(\bar{T}_i)\in\mathbb{R}^m$, repeating the above process step by step, we obtain $((\bar{\alpha},\bar{\beta},\hat{u})^T,X)\in C^0([t_i,t_{i+1}];L^2(0,1);\mathbb{R}^3)\times C^0([t_i,t_{i+1}];\mathbb{R}^m)$. Recalling the transformations (15), (16), (23), (27), (C.1), (C.2), Proposition 1 is thus obtained.

Case 2: With the delay-adaptive control input U_d (61a), the only difference from Case 1 is that the left boundary condition of $\hat{u}$ becomes

$$\begin{aligned}\hat{u}(0,t)=&-\int_0^1\overline{K}_{1z}(y)\bar{\alpha}(y,t)dy-\int_0^1\overline{K}_{2z}(y)\bar{\beta}(y,t)dy\\&+\int_0^1\overline{R}_z(y)\hat{u}(y,t)dy-\overline{\eta}_zX(t)+r\left(\sin\left(\omega\left(t-t_z+\frac{\pi}{2\omega}\right)\right)-1\right),\end{aligned}$$

for $t\in[t_z,t_{z+1})$, where $\overline{K}_{1z}(y)=-K_1(0,y;D)e^{\frac{d_1}{q_1}y}$, $\overline{K}_{2z}(y)=-K_2(0,y;D)e^{-\frac{d_4}{q_2}y}$, $\overline{R}_z(y)=-R(0,y;D)$, $\overline{\eta}_z=-\eta(0;D)$. This difference introduces an additional term $r(\sin(\omega(t^*+\frac{\pi}{2\omega}))-1)$, which is well-defined, into $s(t_z+t^*)$ in (C.16) (replacing $\mathscr{K}$, $\mathscr{R}$, η by $\overline{K}$, $\overline{R}$, $\overline{\eta}$). Therefore, $s(t_z+t^*)$ is still well-defined, and thus well-posedness result in Case 1 still holds.

D. Norms equivalence between the original and the target systems' states

From (13)–(16), (27), (32), we get

$$\|\alpha(\cdot,t)\|^2\leq\eta_1\left(\|z(\cdot,t)\|^2+\|w(\cdot,t)\|^2+|X(t)|^2\right), \tag{D.1}$$

$$\|\beta(\cdot,t)\|^2\leq\eta_2\left(\|z(\cdot,t)\|^2+\|w(\cdot,t)\|^2+|X(t)|^2\right), \tag{D.2}$$

$$\|z(\cdot,t)\|^2\leq\eta_3\left(\|\alpha(\cdot,t)\|^2+\|\beta(\cdot,t)\|^2+|X(t)|^2\right), \tag{D.3}$$

$$\|w(\cdot,t)\|^2\leq\eta_4\left(\|\alpha(\cdot,t)\|^2+\|\beta(\cdot,t)\|^2+|X(t)|^2\right), \tag{D.4}$$

$$\|u(x,t)\|^2\leq\eta_5\|\hat{u}(x,t)\|^2, \tag{D.5}$$

$$\|\hat{u}(x,t)\|^2\leq\eta_6\|u(x,t)\|^2, \tag{D.6}$$

where

$$\eta_1=4\left(1+\int_0^1\int_0^x\phi(x,y)^2dydx+\int_0^1\int_0^x\varphi(x,y)^2dydx+\int_0^1\gamma(x)^2dx\right),$$

$$\begin{aligned}\eta_2 =&4\Bigg(1+\int_0^1\int_0^x \Psi(x,y)^2dydx+\int_0^1\int_0^x \Phi(x,y)^2dydx\\&+\int_0^1 \lambda(x)^2dx\Bigg),\\ \eta_3 =&4\Bigg(1+\int_0^1\int_0^x \bar{\phi}(x,y)^2dydx+\int_0^1\int_0^x \bar{\varphi}(x,y)^2dydx\\&+\int_0^1 \bar{\gamma}(x)^2dx\Bigg),\\ \eta_4 =&4\Bigg(1+\int_0^1\int_0^x \bar{\Psi}(x,y)^2dydx+\int_0^1\int_0^x \bar{\Phi}(x,y)^2dydx\\&+\int_0^1 \bar{\lambda}(x)^2dx\Bigg),\\ \eta_5 =&2\Bigg(1+\int_0^1\int_x^1 R(x,y)^2dydx\Bigg),\\ \eta_6 =&2\Bigg(1+\int_0^1\int_x^1 P(x,y)^2dydx\Bigg).\end{aligned}$$

Recalling (23), together with (D.1), (D.2), (D.5), (D.6), yields

$$\begin{aligned}||v(\cdot,t)||^2 \leq& 4\Bigg(\eta_5+\int_0^1\int_0^1 K_1(x,y)^2dydx\\&+\int_0^1\int_0^1 K_2(x,y)^2dydx+\int_0^1 \eta(x)^2dx\Bigg)\left(||\hat{u}(\cdot,t)||^2\right.\\&\left.+||\alpha(\cdot,t)||^2+||\beta(\cdot,t)||^2+|X(t)|^2\right), \qquad \text{(D.7)}\end{aligned}$$

$$\begin{aligned}||\hat{u}(\cdot,t)||^2 \leq& 4\eta_6(\eta_1+\eta_2+1)\Bigg(1+\int_0^1\int_0^1 K_1(x,y)^2dydx\\&+\int_0^1\int_0^1 K_2(x,y)^2dydx+\int_0^1 \eta(x)^2dx\Bigg)\left(||v(\cdot,t)||^2\right.\\&\left.+\|z(\cdot,t)\|^2+\|w(\cdot,t)\|^2+|X(t)|^2\right). \qquad \text{(D.8)}\end{aligned}$$

Defining

$$\bar{\Omega}(t)=\|\alpha[t]\|^2+\|\beta[t]\|^2+\|\hat{u}[t]\|^2+X(t)^2 \qquad \text{(D.9)}$$

one obtains

$$\xi_1\Omega(t)\leq\bar{\Omega}(t)\leq\xi_2\Omega(t) \qquad \text{(D.10)}$$

where

$$\begin{aligned}\xi_1 =&1/\Bigg(1+\eta_3+\eta_4+4\eta_5+4\int_0^1\int_0^1 K_1(x,y)^2dydx\\&+4\int_0^1\int_0^1 K_2(x,y)^2dydx+4\int_0^1 \eta(x)^2dx\Bigg), \qquad \text{(D.11)}\\ \xi_2 =&1+\eta_1+\eta_2\\&+4\eta_6(\eta_1+\eta_2+1)\Bigg(1+\int_0^1\int_0^1 K_1(x,y)^2dydx\\&+\int_0^1\int_0^1 K_2(x,y)^2dydx+\int_0^1 \eta(x)^2dx\Bigg). \qquad \text{(D.12)}\end{aligned}$$

References

[1] T. Ahmed-Ali, I. Karafyllis and F. Lamnabhi-Lagarrigue, "Global exponential sampled-data observers for nonlinear systems with delayed measurements," *Syst. Control Lett.*, 62, pp. 539–549, 2013.

[2] H. Anfinsen, M. Diagne, M., O. M. Aamo and M. Krstic "An adaptive observer design for $n+1$ coupled linear hyperbolic PDEs based on swapping", *IEEE Trans. Autom. Control*, 61(12), pp 3979-3990, 2016.

[3] H. Anfinsen, M. Diagne, M., O. M. Aamo and M. Krstic "Estimation of boundary parameters in general heterodirectional linear hyperbolic systems", *Automatica*, 79, pp 185-197, 2017.

[4] H. Anfinsen, H. Holta, and O. M. Aamo, "Adaptive control of a scalar 1-D linear hyperbolic PDE with uncertain transport speed using boundary sensing," 2020 American Control Conference (ACC). IEEE, 2020.

[5] H. Anfinsen, H. Holta, and O. M. Aamo, "Adaptive control of a linear hyperbolic PDE with uncertain transport speed and a spatially varying coefficient," 2020 28th Mediterranean Conference on Control and Automation (MED). IEEE, 2020.

[6] H. Anfinsen, and O.M. Aamo, *Adaptive Control of Hyperbolic PDEs*, 2019. Springer.

[7] J. Auriol, F. Di Meglio, and F. Bribiesca-Argomedo, "Delay robust state feedback stabilization of an underactuated network of two interconnected PDE systems," *American Control Conference* 2019.

[8] J. Auriol , U. J. F. Aarsnes , P. Martin and F. Di Meglio "Delay-robust control design for two heterodirectional linear coupled hyperbolic PDEs," *IEEE Trans. Autom. Control*, pp. 3551-3557, vol. 63, no. 10, 2018.

[9] N. Bekiaris-Liberis, M. Jankovic and M. Krstic,"Adaptive stabilization of LTI systems with distributed input delay," *Int. J. Adapt. Control Signal Process*, 27, pp. 46–65, 2013.

[10] P. Bernard and M. Krstic, "Adaptive output-feedback stabilization of non-local hyperbolic PDEs," *Automatica*, 50, pp. 2692–2699, 2014.

[11] D. Bresch-Pietri and M. Krstic, "Delay-adaptive predictor feedback for systems with unknown long actuator delay," *IEEE Trans. Autom. Control*, 55(9), pp. 2106-2112, 2010.

[12] D. Bresch-Pietri and M. Krstic, "Delay-adaptive control for nonlinear systems," *IEEE Trans. Autom. Control*, 59(5), pp. 1203–1218, 2014.

[13] F. Cacace, A. Germani and C. Manes, "An observer for a class of nonlinear systems with time varying observation delay," *Syst. Control Lett.*, 59(5), pp. 305–312, 2010.

[14] X. Cai and M. Diagne, "Boundary control of nonlinear ODE/wave PDE systems with a spatially varying propagation speed," *IEEE Transactions on Automatic Control*, 66(9), pp. 4401–4408, 2020.

[15] J.M. Coron, R. Vazquez, M. Krstic and G. Bastin, " Local exponential H^2 stabilization of a 2×2 quasilinear hyperbolic system using backstepping," *SIAM J. Control Optim.*, 51(3), pp. 2005–2035, 2013.

[16] M.A. Davo, D. Bresch-Pietri, C. Prieur and F. Di Meglio, "Stability analysis of a 2×2 linear hyperbolic system with a sampled-data controller via backstepping method and looped-functionals," *IEEE Trans. Autom. Control*, 64(4), pp.1718–1725, 2018.

[17] J. Deutscher, "Finite-time output regulation for linear 2×2 hyperbolic systems using backstepping," *Automatica*, 75, pp. 54–62, 2017.

[18] M. Diagne., N. Bekiaris-Liberis, A. Otto and M. Krstic, "Control of Transport PDE/Nonlinear ODE Cascades With State-Dependent Propagation Speed," *IEEE Trans. Autom. Control*, 62(12), pp. 6278–6293, 2017.

[19] M. Diagne., N. Bekiaris-Liberis, A. Otto and M. Krstic, "Compensation of input delay that depends on delayed input," *Automatica*, 85, pp. 362-373, 2017.

[20] A. Diagne, M. Diagne, S.-X. Tang and M. Krstic, "Backstepping stabilization of the linearized Saint-Venant-Exner model," *Automatica*, 76, pp. 345–354, 2017.

[21] M. Diagne, S.-X. Tang, A. Diagne and M. Krstic, "Control of shallow waves of two unmixed fluids by backstepping," *Annual Reviews in Control*, 44, pp. 211-225, 2017.

[22] N. Espitia, "Observer-based event-triggered boundary control of a linear 2×2 hyperbolic systems," *Syst. Control Lett.*, pp. 104668, vol. 138, 2020.

[23] N. Espitia, A. Girard, N. Marchand, and C. Prieur, "Event-based boundary control of a linear 2×2 hyperbolic system via backstepping approach," *IEEE Trans. Autom. Control*, pp. 2686–2693, 63(8), 2018.

[24] A. Germani, C. Manes and P. Pepe, "A new approach to state observation of nonlinear systems with delayed output," *IEEE Trans. Autom. Control*, 47(1), pp. 96–101, 2002.

[25] B. Z. Guo and C. Z. Xu, "Boundary output feedback stabilization of a one-dimensional wave equation system with time delay," *17th IFAC World Congress*, 41(2), pp. 8755–8760, 2008.

[26] P. Goatin, "The Aw-Rascle vehicular traffic flow model with phase transitions," *Math. Comput. Model.*, 44, pp. 287–303, 2006.

[27] A. Hasan, O. Aama and M. Krstic, "Boundary observer design for hyperbolic PDE-ODE cascade systems," *Automatica*, 68, pp. 75–86, 2016.

[28] A. Hasan and L. Imsland, "Moving horizon estimation in managed pressure drilling using distributed models," in *Proceedings of the IEEE conference on control applications*, Antibes, France, 2014.

[29] H. Hochstadt, *Integral Equations*, New York, NY, USA: Wiley, 1973

[30] L. Hu, F. Di Meglio, R. Vazquez and M. Krstic, "Control of homodirectional and general heterodirectional linear coupled hyperbolic PDEs," *IEEE Trans. Autom. Control*, 61(11), pp. 3301–3314, 2016.

[31] I. Karafyllis, M. Kontorinaki and M. Krstic, "Adaptive control by regulation-triggered batch least squares," *IEEE Trans. Autom. Control*, 65(7), pp. 2842–2855, 2020.

[32] I. Karafyllis and M. Krstic, "Adaptive certainty-equivalence control with regulation-triggered finite-time least-squares identification," *IEEE Trans. Autom. Control*, 63, pp. 3261–3275, 2018.

[33] I. Karafyllis, M. Krstic and K. Chrysafi, "Adaptive boundary control of constant-parameter reaction-diffusion PDEs using regulation-triggered finite-time identification," *Automatica*, 103, pp. 166–179, 2019.

[34] S. Koga, D. Bresch-Pietri and M. Krstic, "Delay compensated control of the Stefan problem and robustness to delay mismatch," *International Journal of Robust and Nonlinear Control*, 30, pp. 2304–2334, 2020.

[35] M. Krstic, *Delay Compensation for Nonlinear, Adaptive, and PDE Systems*, Springer, 2009.

[36] M. Krstic, "Control of an unstable reaction-diffusion PDE with long input delay," *Syst. Control Lett.*, 58, pp. 773–782, 2009.

[37] M. Krstic and A. Smyshlyaev, "Backstepping boundary control for first-order hyperbolic PDEs and application to systems with actuator and sensor delays," *Syst. Control Lett.*, 57(9), pp. 750–758, 2008.

[38] M. Krstic, "Dead-time compensation for wave/string PDEs," *ASME Journal of Dynamic Systems, Measurement and Control*, 133(3), 031004, 2011.

[39] M. Krstic and D. Bresch-Pietri, "Delay-adaptive full-state predictor feedback for systems with unknown long actuator delay," In *American control conference*, pp. 4500–4505, 2009.

[40] P.-O. Lamare and N. Bekiaris-Liberis, "Control of 2×2 linear hyperbolic systems: backstepping-based trajectory generation and PI-based tracking," *Syst. Control Lett.*, 86, pp. 24–33, 2015.

[41] H. Lhachemi, C. Prieur, and E. Trelat, "PI regulation of a reaction-diffusion equation with delayed boundary control," *IEEE Trans. Autom. Control*, 66(4), pp. 1573-1587, 2020.

[42] H. Lhachemi, C. Prieur, and E. Trelat, "Feedback stabilization of a class of diagonal infinite-dimensional systems with delay boundary control," *IEEE Trans. Autom. Control*, 66(1), pp. 105-120, 2020.

[43] F. Di Meglio, F. Bribiesca-Argomedo, L. Hu and M. Krstic, " Stabilization of coupled linear heterodirectional hyperbolic PDE-ODE systems," *Automatica*, 87, pp. 281–289, 2018.

[44] F. Di Meglio, R. Vazquez and M. Krstic, "Stabilization of a system of $n+1$ coupled first-order hyperbolic linear PDEs with a single boundary input," *IEEE Trans. Autom. Control*, 58, pp. 3097–3111, 2013.

[45] C. Prieur and J. Winkin, "Boundary feedback control of linear hyperbolic systems: Application to the Saint-Venant-Exner equations," *Automatica*, 89, pp. 44–51, 2018,

[46] C. Prieur, J. Winkin and G. Bastin, "Robust boundary control of systems of conservation laws," *Math. Control Signals Syst.*, 20, pp. 173–197, 2008.

[47] J. Qi, S. Dubljevic and W. Kong, "Output feedback compensation to state and measurement delays for a first-order hyperbolic PIDE with recycle," *Automatica*, 128, 109565, 2021.

[48] J. Qi and M. Krstic, "Compensation of spatially varying input delay in distributed control of reaction-diffusion PDEs," *IEEE Trans. Autom. Control*, 66(9), pp. 4069–4083, 2020.

[49] J. Qi, S. Mo and M. Kstric, "Delay-compensated distributed PDE control of traffic with connected/automated vehicles," *IEEE Trans. Autom. Control*, DOI: 10.1109/TAC.2022.3174032, 2022.

[50] J. Qi , S. Wang, J. A. Fang and M. Diagne, "Control of multi-agent systems with input delay via PDE-based method," *Automatica*, 106, pp. 91–100, 2019.

[51] S. X. Tang and M. Krstic, "Sliding mode control to the stabilization of a linear 2×2 hyperbolic system with boundary input disturbance," *American Control Conference*, pp: 1027–1032, 2014.

[52] R. Vazquez, M. Krstic and J. M. Coron, "Backstepping boundary stabilization and state estimation of a 2×2 linear hyperbolic system," *In 50th IEEE Conference on Decision and Control and European Control Conference (CDC-ECC),* pp. 4937–4942, 2011.

[53] J. Wang and M. Krstic, "Vibration suppression for coupled wave PDEs in deep-sea construction," *IEEE Trans. Contr. Syst. Technol.*, 29 (4), pp. 1733–1749, 2020.

[54] J. Wang and M. Krstic, "Delay-compensated control of sandwiched ODE-PDE-ODE hyperbolic systems for oil drilling and disaster relief," *Automatica*, 120, 109131, 2020.

[55] J. Wang and M. Krstic, "Event-triggered output-feedback backstepping control of sandwich hyperbolic PDE systems," *IEEE Trans. Autom. Control*, 67 (1), pp. 220–235, 2021.

[56] J. Wang and M. Krstic, "Regulation-triggered adaptive control of a hyperbolic PDE-ODE model with boundary interconnections," *International Journal of Adaptive Control and Signal Processing*, 35(8), pp. 1513–1543, 2021.

[57] J. Wang and M. Krstic, "Delay-compensated event-triggered boundary control of hyperbolic PDEs for deep-sea construction," *Automatica*, 138, 110137, 2022.

[58] J. Wang and M. Krstic, "Event-triggered adaptive control of coupled hyperbolic PDEs with piecewise-constant inputs and identification," *IEEE Trans. Autom. Control*, 68(3), pp. 1568–1583, 2022.

[59] J. Wang, M. Krstic and I. Karafyllis, "Adaptive regulation-triggered control of hyperbolic PDEs by batch leasts-quares," *American Control Conference*, pp. 4057–4062, 2021.

[60] J. Wang, Y. Pi and M. Krstic, "Balancing and suppression of oscillations of tension and cage in dual-cable mining elevators," *Automatica*, 98, pp. 223–238, 2018.

[61] S. Wang, M. Diagne and J. Qi, "Delay-adaptive predictor feedback control of reaction advection diffusion PDEs with a delayed distributed input," *IEEE Trans. Autom. Control*, 67(7), pp. 3762-3769, 2021.

[62] S. Wang, J. Qi, and M. Diagne, "Adaptive boundary control of reaction-diffusion PDEs with unknown input delay," *Automatica*, 134, 109909, 2021.

[63] S. Wang, J. Qi and M. Krstic, "Delay-adaptive control of first-order hyperbolic PIDEs," *arXiv preprint arXiv:2307.04212*, 2023.

[64] H. Yu and M. Krstic, "Traffic congestion control for Aw-Rascle-Zhang model," *Automatica*, 100, pp. 38–51, 2019.

[65] L. Zhang and C. Prieur, "Necessary and sufficient conditions on the exponential stability of positive hyperbolic systems," *IEEE Trans. Autom. Control*, 62, pp. 3610–3617, 2017.

[66] Y. Zhu and M. Krstic, "Adaptive backstepping control of uncertain linear systems under unknown actuator delay," *Automatica*, 59, pp. 256–265, 2015.

[67] Y. Zhu, M. Krstic, and H. Su, "Adaptive output feedback control for uncertain linear time-delay systems," *IEEE Trans. Autom. Control*, 62(2), 545–560, 2017.

Ji Wang is currently an Associate Professor in the Department of Automation at Xiamen University, Xiamen, Fujian, China. He received the Ph.D. degree in Mechanical Engineering in 2018 from Chongqing University, Chongqing, China. From 2019 to 2021, He was a Postdoctoral Scholar in the Department of Mechanical and Aerospace Engineering at University of California, San Diego, La Jolla, CA, USA. He has co-authored (with M. Krstic) the book entitled *PDE Control of String-Actuated Motion* (Princeton University Press). Since 2021, he serves as an Associate Editor of Systems & Control Letters. His research interests include modeling and control of distributed parameter systems.

Mamadou Diagne holds the position of Assistant Professor with the Department of Mechanical and Aerospace Engineering at the University of California San Diego, with an affiliation to the Department of Electrical and Computer Engineering. He completed his Ph.D. in 2013 at the Laboratory of Control and Chemical Engineering of the University Claude Bernard Lyon I in Villeurbanne (France). Between 2017 and 2022, he was an Assistant Professor with the Department of Mechanical Aerospace and Nuclear Engineering at Rensselaer Polytechnic Institute. From 2013 to 2016, he was a Postdoctoral Scholar first at the University of California San Diego and then at the University of Michigan. His research focuses on the control of partial differential equations (PDEs) and delay systems as well as coupled PDEs and nonlinear ordinary differential equations with a particular emphasis on adaptive control, sampled-data control and event-triggered control. His expertise extends to controlling fluid and flow dynamics to manage water systems, traffic systems, supply chain dynamics, additive manufacturing processes and extrusion-based processes. He serves as Associate Editor for Automatica and Systems & Control Letters. He received the NSF Career Award in 2020.